SEPARATION OF PROTEINS BY ION EXCHANGE AND MEMBRANE CHROMATOGRAPHY: BUFFER COMPOSITION, INTERFERING IMPURITIES AND FOULING CONSIDERATIONS

A Thesis

by

TAHMINA IMAM

Submitted to the Office of Graduate Studies of
Texas A&M University
in partial fulfillment of the requirements for the degree of

MASTER OF SCIENCE

May 2009

Major Subject: Chemical Engineering

SEPARATION OF PROTEINS BY ION EXCHANGE AND MEMBRANE CHROMATOGRAPHY: BUFFER COMPOSITION, INTERFERING IMPURITIES AND FOULING CONSIDERATIONS

A Thesis

by

TAHMINA IMAM

Submitted to the Office of Graduate Studies of
Texas A&M University
in partial fulfillment of the requirements for the degree of

MASTER OF SCIENCE

Approved by:

Chair of Committee,	Zivko Nikolov
Committee Members,	Mahmoud El-Halwagi
	Daniel Shantz
Head of Department,	Michael Pishko

May 2009

Major Subject: Chemical Engineering

ABSTRACT

Separation of Proteins by Ion Exchange and Membrane Chromatography: Buffer Composition, Interfering Impurities and Fouling Considerations.

(May 2009)

Tahmina Imam, B.S., San Jose State University

Chair of Advisory Committee: Dr. Zivko Nikolov

Efficient separation of target protein from impurities is crucial in bioseparation for large scale production and purity of the target protein. Two separation process approaches were considered in this study. The first approach focused on identifying major impurity and optimization of solution properties for target protein purification. The second approach consisted of designing an adsorbent that interacted specifically with the target molecule. The first study included modification of protein solution properties (pH, ionic strength, buffer ions) in order to maximize lysozyme purification by a strong cation exchange resin. The interaction of phytic acid, a major impurity, present in transgenic rice extracts, that contributes to decreased lysozyme adsorption capacity on SP Sepharose was evaluated. The target protein was lysozyme, which is used in a purified form as a baby formula additive to reduce gastrointestinal tract infections. At constant ionic strength, lysozyme in pH 4.5 acetate buffer had a higher binding capacity and stronger binding strength than at pH 6.0. Lysozyme in sodium phosphate buffer of pH 6.0 exhibited lower adsorption capacity than in pH 6 Tris buffer. Binding capacity and strength were significantly affected by phytic acid in all studies buffers. The second study consisted of surface modification of microfiltration membranes for protein purification and separation and reduces fouling. This study describes adsorption and fouling of chemically modified microfiltration membranes with bovine serum albumin (BSA) and immunoglobulin G (IgG). Least fouling resulted with polyethylene glycol (PEG) membranes when BSA protein was used. Amine-functionalized membranes showed specific interaction with BSA. There was multi-layer deposition of IgG on amine-functionalized membrane. G3

membrane synthesized to selectively bind IgG seemed a noble option to separate IgG from a protein mixture.

TABLE OF CONTENTS

Page

CHAPTER Page

LIST OF FIGURES

FIGURE Page

LIST OF TABLES

CHAPTER I

INTRODUCTION

1.1 Thesis Organization

This thesis has four chapters. Chapter I is a general introduction which consists of the hypotheses and objectives, literature review on the sources and functions of lysozyme, phytic acid and its interaction with proteins, membrane processes and purification of IgG proteins. Chapter II presents the study of the effects of phytic acid on binding capacity of lysozyme. Chapter III describes adsorption and fouling of chemically modified microfiltration membranes with BSA and IgG. Finally, Chapter IV offers a general conclusion to the entire work and discusses future directions of this work.

1.2 Hypotheses and Objectives

The research described in this thesis was undertaken to test 4 hypotheses relating to the phytic acid effect on binding capacity of lysozyme on cation exchange and the fouling of microfiltration membranes by proteins.

The hypotheses are as follows:

- Determination of the best conditions; buffer composition and pH can improve purification process; adsorption capacity of lysozyme.
- Removal of rice impurity; phytic acid from rice extract can improve purification yield and specific activity of lysozyme.
- Microfiltration (MF) for protein purification is expected to have lower processing cost and higher throughput if fouling can be minimized.
- IgG1 can be specifically adsorbed and eluted from Protein A-mimetic membranes

---

This thesis follows the style of *Biotechnology Progress.*

The objectives of this research were:

- To investigate the effect of buffer composition and pH on the adsorption capacity of lysozyme.
- To investigate the effect of phytic acid impurity present in rice extracts on adsorption capacity of lysozyme.
- To chemically modify microfiltration alumina membranes to reduce protein fouling.
- To develop novel microfiltration membranes for affinity separation of IgG from protein mixtures.

1.3 Literature Review

1.3.1 Transgenic plants as hosts for recombinant protein production

Transgenic plants as bioreactors have various advantages in expressing and producing recombinant biomolecules. They offer low upstream production cost as these bioreactors require only light, water, carbon dioxide and minerals. The ease in production scale up, low capital investment, and minimal risk of contamination with mammalian viruses in contained environment is many of the advantages of using transgenic plants as bioreactors (*1*). To lessen the probability of mammalian viral vectors, usage of transgenic plants has been considered for large scale recombinant protein production (*2*).

Various crops corn, potato, canola, sunflower, soybean, tobacco, rice etc. have been used for the expression of human biopharmaceuticle and antibodies (*3*). Canola and corn has been mostly used for expressing acidic recombinant proteins, while soybean has been in use for expressing basic recombinant proteins (*4*). Cereal crops such as rice have been popular for expressing human proteins due to its long term storage capacity and low phenolics concentration, which may cause problems in the purification of tobacco and other leaf-tissue-derived recombinant proteins (*2, 5, 6*). Also, using transgenic rice for recombinant lysozyme expression has the advantage over other systems, e.g., *Aspergillus,*

Saccharomyces or tobacco, because of less stringent purification requirements for oral formulation of recombinant product (*7*).

Rice based foods are considered hypoallergenic (*8*) thus, human lysozyme produced from transgenic rice could have many important applications. Studies have shown that lysozyme expressed by transgenic rice was able to protect intestinal tract similarly to subtherapeutic antibiotics (bacitracin, roxarsone, antibiotics) (*7*). Such recombinant lysozyme was able to reduce bacterial infections and decrease proinflammatory cytokines (*7, 8*). Therefore, human lysozyme expressed from transgenic rice could be used in a partially purified form as a baby formula additive to provide defense against bacteria along epithelial surfaces (*2, 9, 10*). These molecules are highly resistant to hydrolysis by acids and proteases and to digestion in the gastrointestinal tract (*7, 11-14*).

1.3.2 Phytic acid, presence in rice and other grain seeds

Recombinant lysozyme expressed from rice flour contain phytic acid, an impurity that could be detrimental to purification efficiency and/or product activity if interact with proteins (*15-17*). Phytic acid is present at a higher amount than other impurities, i.e. 1 mg/g in brown rice (*15*) and is also found within the hulls of nuts, seeds, and grains (*18*). Phytic acid is a strong chelator of important minerals such as calcium, magnesium, iron, and zinc, and can therefore contribute to mineral deficiencies in people whose diets rely on these foods for their mineral intake (*18*). Figure 1.1 shows a structure of phytic acid.

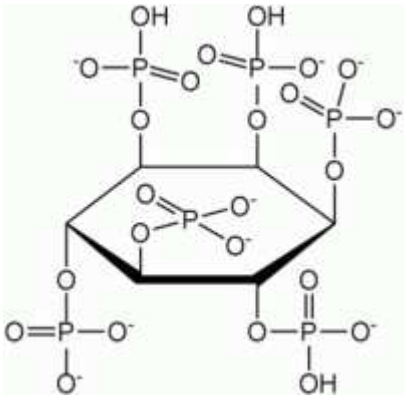

Figure 1.1 Structure of phytic acid. *(17)*

Phytic acid molecule contains 12 dissociable hydrogens and depending on the pH of the solution different phytic acid anions may be formed having different degree of protonation (*19, 20*). Several studies have shown the involvement of side chains of proteins in the formation of protein-phytic acid complexes. For proteins at pH lower than isoelectric point, the terminal amino, lysil, histidyl arginyl groups can be positively charged and form complex with a negatively charged phytate anion (*16, 21*). With an increase in the pH, the interaction between phytic acid and protein is decreased.

Phytic acid forms both binary and tertiary complexes with positively charged proteins. Work by Cheryan (*16*) on the removal of phytic acid from soy extracts indicates that such complexes are difficult to break and remove phytic acid by ultra-filtration or difiltration. Therefore, binary and tertiary complexes of lysozyme and phytic acid are likely to be present in rice extracts and affect lysozyme adsorption on cation ion exchange resins. Identification of such complexes and their role in reducing the protein adsorption capacity remains a challenge.

1.3.3 Lysozyme and applications

Lysozyme consists of 129 amino acid residues that have a molecular weight of approximately 14.7 kDa (*22*). It catalyzes hydrolysis of 1,4-beta-linkages between N-acetylmuramic acid and N-acetyl-D-glucosamine residues in peptidoglycan and between N-acetyl-D-glucosamine residues in chitodextrins (*22, 23*). The catalytic activity of lysozyme is non-specifically targeted to the bacterial cell membranes and related with general non-specific organism defense (*22, 24*). Lysozyme can be found in the mucosal secretion such as saliva, tears and breast milk (*24*) and about 3% in chicken egg-white (*22, 25*). This enzyme is only effective against gram positive bacterial cells. Gram negative bacteria and yeast are completely resistant to lyses by it (*22, 24*). Due to limited supply from human sources and risk of viral contamination, transgenic plants usage has been popular in the production of recombinant lysozyme as discussed under section 1.3.1 (*24*).

Lysozyme was first discovered in 1922 by Alexander Fleming, who found it in human nasal secretion (*22*). In 1965 the structure of lysozyme was solved by X-Ray analysis with 2 angstrom resolution by David Chilton Phillips. For many years lysozyme has been the best object for X-Ray analysis due to many unique properties; easy purification and crystallization from egg-white of this enzyme, a feature that is widely used for its' purification (*22*). Currently, lysozyme crystals were known to have the highest resolution structure presented in Protein Data Bank that was solved at resolution 0.94 Angstrom when diffracted X-Ray beam (*22, 23*).

Lysozyme is well known for increasing the natural defenses of the body against bacterial infections (*26*). There are various pharmaceutical applications of lysozyme; sore throats and canker sores treatment by lozenges, decontamination of contact lenses with eye drop solution (*24*). Lysozyme is also added to infant formulae in order to make them more closely resemble to human milk (*25*). Lysozyme is used to prevent a problem known as 'butyric late blowing', which occurs during the ripening of certain European-type cheeses. This problem occurs from the contamination of milk by a naturally occurring, spore-forming bacterium, called *Clostridium tyrobutyricum*. The origin of the contamination of milk by this bacterium lies in the widespread use of silage as a feed (*24*).

1.3.4 Membrane technology in protein purification

Membrane separation methods exploit different characteristics of the influent stream and the membrane and can be categorized into separations based on size (0.0001 to 100 μm) and separation based on specific interactions, i.e. ionic, hydrophobic, and affinity. Various types of these membrane separations that have been developed for specific industrial applications include microfiltration (sterile filtration, clarification), ultrafiltration (separation of macromolecular solutions), nanofiltration (removal of hardness and desalting), reverse osmosis (separation of salts and microsolutes from solutions), electrodialysis (desalting of ionic solutions), gas separation (separation of gas mixtures), and pervaporation (separation of azeotropic mixtures) (*32, 33*).

In recent years, a great deal of attention has been paid to microfiltration (MF) and ultrafiltration (UF) for protein purification because it is expected to ultimately have lower processing cost and higher throughput (*34-44*). The main distinction between MF and UF is that ultrafiltration membrane retains much smaller particles from the passage through the membrane than do microfiltration membranes. Typically the particle size is measured by molecular weight, and ultrafiltration membranes have retention ranges from 1,000 to 1,000,000 Da in nominal molecular weight. UF membranes have pore size ranging from 0.1 mm to 5 nm (*32*). Inorganic materials such as ceramics, carbon based membranes, zirconia etc. have been commercialized for various applications such as separation and concentration of biologically active components, treatment of whey in dairy (*32*), enzyme and pharmaceutical preparations, concentration of biological macromolecules, electrocoat paint recovery etc. However, microfiltration is by far the most widely used membrane process with total sales greater than the combined sales of other membrane processes (*33*). MF membranes are made from natural or synthetic polymers such as cellulose nitrate or acetate, polyvinylidene difluoride (PVDF), polyamides, polysulfone, polycarbonate, polypropylene, PTFE etc. The inorganic materials such as metal oxides (alumina), glass, zirconia coated carbon etc. are also used for manufacturing the MF membranes.

MF of macromolecular solutions (separating material of colloidal size by a sieving mechanism with distinct pore sizes for retaining larger size particles than the pore diameter) is widely used in the biotechnological industries involved in separation and purification of proteins from complex mixtures through porous membranes with typical pore diameters on the order of 0.1 – 0.6 μm (*45, 48*). Figure 1.2 shows an illustration of microfiltration membrane. Typical uses of microfiltration via ceramic membranes include primary cell recovery from fermentation broths and sterile filtration as the final step in the production of a protein product (*46*), preparation of parenterals and sterile water for pharmaceutical industry (*47*), concentration of fruit juices and alcoholic beverages in food & beverage industry (*32, 33*), waste treatment for removing intractable particles in oily fluids, aqueous wastes which contain particulate toxics and stack gas (*32*).

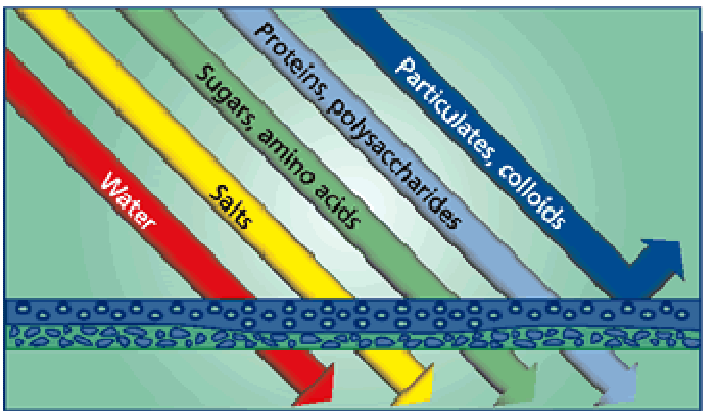

Figure 1.2 Microfiltration illustration. (*30*)

1.3.5 Protein purification by chromatography

Various proteins of interest are purified by chromatography for their applications in industry every day. Chromatography separates compounds on the basis of their charge, size, shape, and solubility (*28, 29*). There is a mobile phase (consisting of solvent and the molecules to be separated) and a stationary phase (resin) through which the mobile phase travels. Molecules travel through the stationary phase at different rates because of their interaction chemistry (*28*). Proteins may be separated based on their size (gel filtration chromatography) affinity for a specific ligand molecule such as an antibody (affinity chromatography), and opposite charge interaction between a protein and stationary phase (ion exchange chromatography (*29*).

Ion-exchange chromatography separates molecules based on their charged groups, which cause the molecules to interact electrostatically with opposite charges on the stationary-phase matrix (*28*). Ion exchange chromatography is commonly used for lysozyme purification. .where positively charged lysozyme binds to the negatively-charged groups on the stationary phase and the bound protein is then eluted from the column using a salt (*28*). Different types of molecules will bind to the matrix with affinities that depend on both the conditions used and the types and number of individual charged groups. These differences lead to resolution of various molecule types by ion-exchange chromatography (*28, 29*). Binding capacity and purity of the target proteins may be severely affected if there are impurities present in the protein samples. Therefore, the interaction of the impurities with the resin binding sites and target protein are important factors to improve

the product and purification yield. For an efficient purification process, knowledge of the protein solubility, charge, size, hydrophobicity, biological affinity and protein interaction with impurities should be considered in ion exchange chromatography (*29, 30*).

1.3.6 Membrane adsorbers in downstream separations

Novel application of membranes as adsorbers in protein separation is replacing chromatographic resins in certain applications. In such cases, adsorption kinetics or adsorption isotherms are governed by simple diffusion from protein solutions (*49-51*). Membrane surface chemistry, protein structure, magnitude and sign of charge of both protein and membrane surface and the degree of hydration of the protein are all important factors in determining the amount of protein adsorbed (*46*).

Advantages of membrane adsorbers versus resin compaction in column chromatography in purification and separation is that they expand the allowed range of temperatures and pressures. In comparison to packed bed chromatography, membrane chromatography has a lower pressure drop, higher flow rate, and higher productivity as a result of the microporous/macroporous structure of the thin membrane (*52*). Furthermore, membrane adsorbers are better fit than resins to withstand extreme conditions and reagents that are typically used in biotech industry for cleaning and regenerations and easier to scale-up (*51, 52*).

There have been many applications of protein purification by membrane adsorbers. Thiophilic ligands were coupled onto regenerated cellulose membranes for the purification of monoclonal antibodies by Finger et al. (*53*). Finger studied binding capacities for IgG1 and IgG2 in dead-end and cross-flow filtration mode (*53*). Separation and purification of lysozyme from egg white solution were investigated by affinity membrane absorbers using two different dye-ligands, i.e. Procion Brown MX-5BR (RB-10) and Procion Green H-4G (RG-5) that were immobilized onto poly (2-hydroxyethylmethacrylate) membranes (*54*). Other applications of membrane absorber include purification of plasmid DNA, viral vectors, removal of chromosomal DNA, etc.

Such purification technology has been used by Pall life sciences, Pall Corporation, UK (*55*). Therefore, membrane adsorbers appear to have a promising future in large-scale separation processes for the isolation, purification, and recovery of proteins and other biological.

1.3.7 Membrane fouling

While removal of particles (>20 nm diameter) or other organic matter is achieved by microfiltration membranes, these membranes are susceptible to membrane fouling which limits their use. Membrane fouling causes a loss of membrane permeability that occurs over time and results from an accumulation of material called foulant on the surface and within the porous structure of the membrane during filtration (*56, 57*). Types and amounts of fouling are dependent on many different factors, such as feed solution characteristics (foulants present in feed may be proteins, cell debris, DNA etc), membrane type, membrane materials and process design and control (*57, 58*).

In general, membrane fouling consists of a monolayer or multilayer of macromolecules adsorbed on the membrane surface and on the walls of membrane pores. Macromolecules, denatured and aggregated macromolecules and other feed stream components could also be deposited on the adsorbed monolayer (*58*) or stick to the membrane and act as sites for further fouling buildup (*59*). Hallstrom (*60*) described fouling by protein as a three-step process; first, membrane resistant increases due to reduction in pore size because of deposition of protein particles on the membrane surface and at the entrances to the pores (mostly monolayer adsorption), second deposition occurs on top of the first deposited layer which may consist of protein precipitation, unfolding, aggregation etc. causing a slower rate of increase in the membrane resistance than the initial deposition, third bridging of the pore entrances occurs where a complete surface layer builds up (*60*).

Proteins usually interact with membrane surfaces by a variety of mechanisms including electrostatic attraction, hydrophobic interactions, hydrogen bonding, and van der Waals forces that result in fouling (*48*). Research has shown that fouling decreases with

electrostatic repulsion between protein and membrane due to increase in selectivity (*39, 42, 43*). On the other hand, hydrophilic interaction between protein and membrane reduces adsorption of protein (*48-50*). Salgin (*39*) showed that hydrophobic forces were important in protein adsorption on membrane surfaces. Since most membranes are not hydrophilic, surface modification has been shown to be a promising approach to membrane development to reduce fouling. Fouling illustration in microfiltration membranes is shown in Figure 1.3.

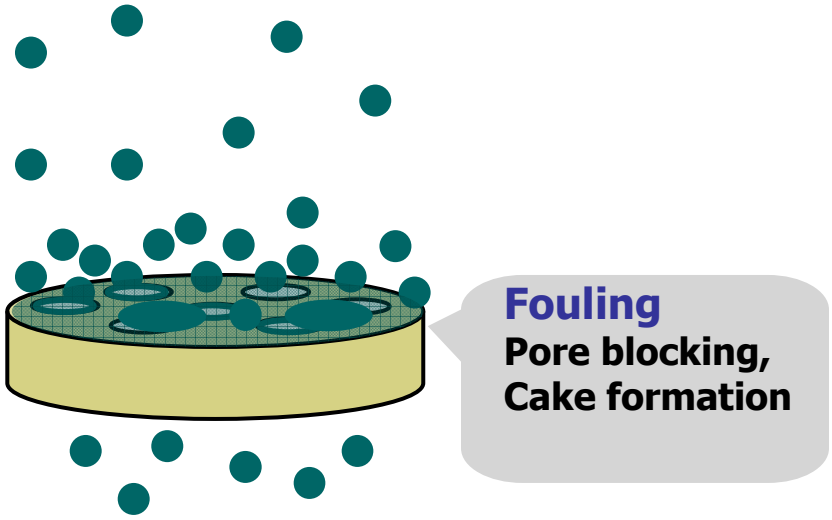

Figure 1.3 Membrane fouling illustration.

Fouling causing a decrease in permeability of membrane would result in lower permeate (filtrate) flow rate (flux) at a given pressure. To maintain permeate flux, higher pressure has to be generated. To improve the processes to lessen fouling has become an important target in industry. Availability of improved membrane surfaces of different properties has provided an important path for increasing throughput and productivity in protein purification (*58, 59*). Usage of inorganic membranes; ceramic/alumina membranes has shown to undergo rapid fouling (*41-43*). However, organic layers synthesized on these membranes reduced fouling (*15*). Therefore, to design hybrid membranes would be a better alternative where features of both ceramic membrane (high pore size uniformity) and designed organic layers on the membranes (potential diversity in surface chemistry) can be integrated to reduce fouling (*34, 49*). This can then ensure getting higher

protein/enzyme permeability, or passage through the membrane to maximize yield and recovery, thus reducing capital costs.

1.3.8 Protein A based purification of monoclonal antibodies (IgG1)

Today's biopharmaceutical industries are dominated by monoclonal antibodies that are utilized as a reagent for detecting pancreas cancer, intestinum crassum cancer and hepatoma (*29, 48, 58, 61-62*). Protein engineering, molecular evolution and other new protein design techniques are increasingly being used to further refine the characteristics and performance of various antibodies (*63*).

In most cases, purification units in a large-scale antibody process must deliver high yield, process reliability and be robust and cost-effective (*48, 64*). There are several large scale antibody purification processes that use immobilized protein A or protein A subdomains as the primary capture and purification step (*48, 63-64*). Figure 1.4 shows a schematic representation of IgG with its Fc and variable domains.

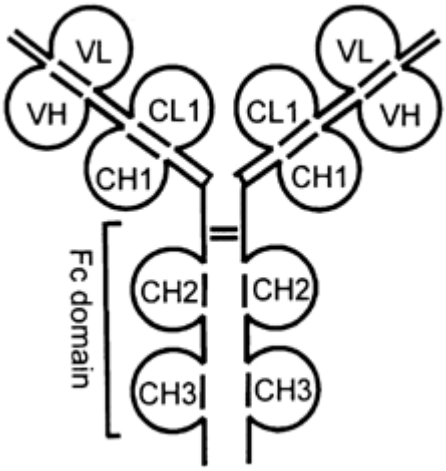

Figure 1.4 Schematic representation of IgG. (*88*)

Fc domain is important for binding to Protein A, which is a cell wall component of *Staphylococcus aureas* consisting of a single polypeptide chain (*65-67*). The C-terminus

of the chain begins with a cell wall/membrane associated region, consisting of a linear series of 5 highly homologous antibody binding domains (*68*) that have equivalent ability for antibody binding. From antibody purification studies, majority of the binding energy comes from hydrophobic interactions (*52, 69*). The strong interaction between Protein A and Fc domain of IgG allows efficient purification of IgG from variety of sources (*63-64, 80*).

CHAPTER II

EFFECTS OF CRITICAL RICE EXTRACT IMPURITY, PHYTIC ACID ON THE DESIGN OF DOWNSTREAM PROCESSING; BINDING CAPACITY OF RECOMBINANT LYSOZYME

2.1 Introduction

Lysozyme is a medicinal agent, used as a hemostatic, anti-inflammatory, tissue regeneration, and anti-tumor therapeutic applications to a variety of human diseases. Its common applications are as a cell disrupting agent for extraction of bacterial intracellular products, antibacterial agent in ophthalmologic preparations, food additive in milk products and drug for treatment of ulcers and infections (*25, 26*). The sources of lysozyme such as breast milk, tears, saliva, and nasal secretion are not adaptable for commercial development due to limited supply, low concentrations in the starting material and possible risk of viral and microbial contamination (*2, 27*). To lessen the probability of mammalian viral vectors, usage of transgenic plants has been considered for large scale recombinant protein production (*25*). Transgenic plants as bioreactors have various advantages in expressing and producing recombinant biomolecules. They offer low upstream production cost as these bioreactors require only light, water, carbon dioxide and minerals. The ease in production scale up, low capital investment, and minimal risk of contamination with mammalian viruses in contained environment is many of the advantages of using transgenic plants as bioreactors.

Recently transgenic rice has been developed by Ventria Bioscience Inc. (http://www.ventria.com) to produce human lysozyme to be used in a purified form as a baby formula additive to reduce gastrointestinal tract infections (*1, 27*). Previous studies by Wilken and Nikolov (*2*) investigated the best conditions for lysozyme extractability and purification by ion exchange chromatography as a function of pH and ionic strength. Highest extracted lysozyme to native protein ratio was obtained at pH 4.5 and 100 mM NaCl in 50 mM sodium acetate buffer (*2*). The best conditions for lysozyme adsorption on a cation exchange resin were pH 4.5 and 50 mM sodium acetate buffer containing 50

mM NaCl. Although high purity was achieved with a single chromatography step by adjusting the pH 4.5 extract to pH 6 before adsorption, drastically lower saturation capacity was a major disadvantage compared to lysozyme adsorption at pH 4.5 (*2*). This difference in adsorption capacity has been ascribed to interference by the extract impurities. Specifically for lysozyme extracted from rice flour, phytic acid and ferrulic acid were hypothesized as possible impurities that could affect lysozyme adsorption capacity.

In ion-exchange chromatography, separation of proteins is obtained by reversible adsorption (*28*). Typically, a protein sample is first applied and adsorbed in a packed-bed-column filled with an ion exchange resin, and the unbound substances are washed out from the column using the starting buffer. Then, the bound proteins are sequentially eluted from the column and separated from each other (*28*). The presence of various impurities in the protein samples could severely affect the binding capacity and purity of the target proteins. Therefore, it is important to understand how these impurities interact with the resin binding sites and target protein in order to improve the product and purification yield. Literature review indicates that phytic acid present in transgenic rice extract, could be detrimental if interacts with lysozyme (*15-17*). Phytic acid is present in a greater amount than other impurities in brown rice (1 mg/g) and it can form binary and tertiary complexes with positively charged proteins (*15*). Work by Cheryan (*16*) on the removal of phytic acid from soy extracts indicates that such complexes are difficult to break and remove phytic acid by ultra-filtration or diafiltration. Therefore, binary and tertiary complexes of lysozyme and phytic acid are likely to be present in rice extracts and affect lysozyme adsorption on cation ion exchange resins. Identification of such complexes and their role in reducing the protein adsorption capacity remains a challenge.

Although a number of studies have been reported, where effects of ionic strength and pH on protein adsorption have been investigated by using different ion exchangers (*28, 30, 31*) other properties such as structural characteristics and charge density of the protein (*28*), impurities and ion exchange resin should also be considered. The knowledge of the different impurities present in rice extract and their interaction with the target protein

and/or resin binding sites will contribute to the development of more efficient purification processes whose costs usually represent a large percentage of overall production costs. The objective of this study is to evaluate the effects of phytic acid and adsorption buffers on lysozyme binding to a strong cation exchange resin.

2.2 Experimental Procedure

2.2.1 Materials

The model protein, lysozyme from hen egg white (HEWLZ) was purchased by (>93% purity) Sigma Chemical Co. (L6876-10G, #096K1237) and used for protein analysis and quantification. Phytic acid dodecasodium salt hydrate was provided by Aldrich (L#035K0590) and used for rice impurity analysis on lysozyme. Cation exchange stationary phase, SP Sepharose FF, was purchased from GE Healthcare, (L#306691) and used as the adsorbent media for the protein. Materials used for equilibration buffer preparation were sodium acetate anhydrous, (EM SCIENCE, L#28735B65, CAS127-09-3), sodium phosphate, dibasic, 12-Hydrate, crystal (J.T. Baker L#Y49582), sodium chloride crystal, ACS (Fisher Scientific, L#974747), TRIS base, (J.T.Baker, #4099-02, CAS #77-86-1). Resin cleaning solutions used were 0.1M sodium hydroxide (EM Science #SX0590-3, L42235240), and RO water and storage solution used was 20% ethanol.

2.2.2 Analytical methods

Analytical balance (Mettler Model) of 0.001g reliability was used to weigh out the protein and phytic acid powder. DU 640 UV Spectrophotometer, (Beckman Coulter) was used to determine initial and final supernatant absorbancies during adsorption equilibrium test. For determining low protein concentrations (below 0.1 g/l) in the supernatant, Bradford method (*71*) with bovine serum albumin as a standard was used.

2.2.3 Experimental methods

2.2.3.1 Equilibrium experiments. Batch adsorption isotherms for HEWLZ were determined as a function of pH, buffer and phytic acid. The isotherms with SP Sepharose

resin were measured by dosing a known volume of adsorbent into a known volume and concentration of protein solution contained in a 20 ml sterile centrifuge tubes. Table 2.1 below shows the different equilibration buffers and conditions used for this study. The conductivity of buffer solutions with or without lysozyme and phytic acid were measured by a conductivity meter (Fisher Scientific).

Table 2.1 Conditions and equilibration buffers used for adsorption isotherm study.

Buffer	pH	Conductivity (mS)	Salt
50 mM Sodium acetate	4.5	9.7	50 mM Sodium chloride
50 mM Sodium acetate	4.5	12.6	73 mM Sodium chloride
50 mM Sodium phosphate	6.0	12.6	50 mM Sodium chloride
50 mM Tris	6.0	12.6	90 mM Sodium chloride

Equilibrium experiments with only lysozyme or with a mixture of lysozyme and phytic acid were performed with the conditions stated in Table 2.1. Analytical balance was used to measure the dry weight of HEWLZ powder. One to ten (1:10) molar concentration ratio of HEWLZ to phytic acid solution was prepared for the experiments where phytic acid effect was considered. Previously weighed HEWLZ or HEWLZ and phytic acid were dissolved in predetermined amount of the equilibration buffer to reach thdesired final protein concentration. The total volume sample including the adsorbent was 10 ml. The concentration of HEWLZ in the 10 ml sample was varied from 0.3 to 6.0 mg/ml and protein solution with or without phytic acid mixed for about an hour. The concentration of the prepared HEWLZ solution was then measured by the spectrophotometer at a wavelength of 280 nm. Extinction coefficient used was 2.54 ml/μg.cm (*4*) and the conductivity of each solution was noted.

Adsorption experimentsa were performed in a 15 ml polycarbonate tube containing 1 ml (settled volume) SP Sepharose resin. The resin was added to approximately 10 ml of lysozyme solution and final volume adjusted to 11 ml. Once the resin was added to the lysozyme or lysozyme and phytic acid solution, the tubes were rotated end-over-end for a period of 24 hrs at room temperature using a rotation mixer (Fisher Scientific).

At the end of the equilibration time, the slurry was centrifuged (Centrific, Fisher Scientific) for about 1 minute at room temperature and the protein concentration in the supernatant was determined. All the protein solutions before and after the adsorption experiments were also tested for protein aggregation by measuring the solution absorbance at 420 nm. The protein adsorbed, q* was calculated using the following mass balance:

$$q^* = [(C_o - C^*)q_{t]}/ R \qquad (1)$$

Where,

q* - protein adsorbed (mg/ml)

C_o - concentration of original protein solution (mg/ml)

C* - protein remaining in solution after adsorption (mg/ml)

q_t -total protein volume (ml)

R is resin volume (ml)

Experiments with HEWLZ and phytic acid were performed the same way as above. The experimental equilibrium data were fitted to the Langmuir model to determine the maximum binding capacity, q_m and dissociation constant, K_d.

$$q^* = q_m (c^*) / K_d + c^* \qquad (2)$$

Where,

q* - protein adsorbed (mg/ml)

q_m - maximum binding capacity (mg/ml)

C* - supernatant concentration (mg/ml)

K_d - dissociation constant (mg/ml)

Ionic strength calculation was performed using the following equation:

$$I = ½ \sum Zi^2 [Xi] \qquad (3)$$

Where,

Z - the charge on ion i

X - the molar concentration of i

All equivalent initial concentration, C_o to each supernatant concentration, C*, formation of Aggregates at different pH and buffers are shown in the appendix. Aggregation checked at 420 nm for all the experiments was not significant.

2.2.3.2 Uptake experiments. For HEWLZ uptake experiments, a similar procedure as described above was followed. Once the required HEWLZ or HEWLZ and phytic acid solutions were prepared at the conditions stated in Table 2.1, the decrease in protein adsorption/uptake was measured by UV absorbance at 280 nm every 30 seconds for 5 minutes. . In previous work by Wilken and Nikolov (*2*), pH of human HEWLZ containing rice extract was adjusted from 4.5 to 6.0 to obtain a higher purity during ion-exchange chromatography (*2*). To mimic these conditions, the pH adjustment of HEWLZ or HEWLZ-phytic acid solution from 4.5 to 6.0 was performed. The pH adjustment from 4.5 to 6.0 was performed in 3 different ways by using 1 M sodium phosphate, 0.5 M sodium hydroxide, and 1 M Tris solutions. In all cases, the initial enzyme or enzyme-phytic acid solutions were prepared in sodium acetate buffer of pH 4.5. The pH adjustment were carried out for a period of 25 minutes. Otherwise, uptake experiments were carried out the same way as before. The raw uptake data can be found in the Appendix A.

2.3 Results and Discussion

2.3.1 Effect of pH and buffer on lysozyme adsorption

The amount of lysozyme adsorbed on the cation exchange resin as a function of pH and buffer is shown in Figure 2.1. The conductivity of initial solutions were measured and adjusted to 12.6 mS to eliminate the effect of ionic strength on HEWLZ adsorption. In one case, for the pH 4.5 acetate buffer, the ionic strength was left at 9.7 mS. Two different buffers (Tris and sodium phosphate) and 2 different pH's (4.5 and 6) were compared. The phosphate and Tris buffers were compared at pH of 6.0. The two buffers were: 50 mM sodium phosphate with 50 mM NaCl and 50 mM Tris containing 90 mM NaCl. Ionic strength of both was 0.25 (equation 3).

When using Tris buffer, lysozyme adsorption was 84 mg/ml of resin while using phosphate buffer, lysozyme adsorption was 74 mg/ml of resin (Fig 2.1). In the presence of Tris buffer, lysozyme binding was greater than that in sodium phosphate. Even though, Tris increased binding of lysozyme on SP Sepharose, further studies showed that Tris had

much lower buffering capacity than sodium phosphate. It was difficult to maintain a constant pH when Tris buffer was used. Tris at pH 6.0 has lower buffering capacity than phosphate buffer and a decrease in pH with increase of lysozyme concentration was observed which presumably resulted in higher adsorption. Such pH change was not observed when phosphate or acetate buffers were used.

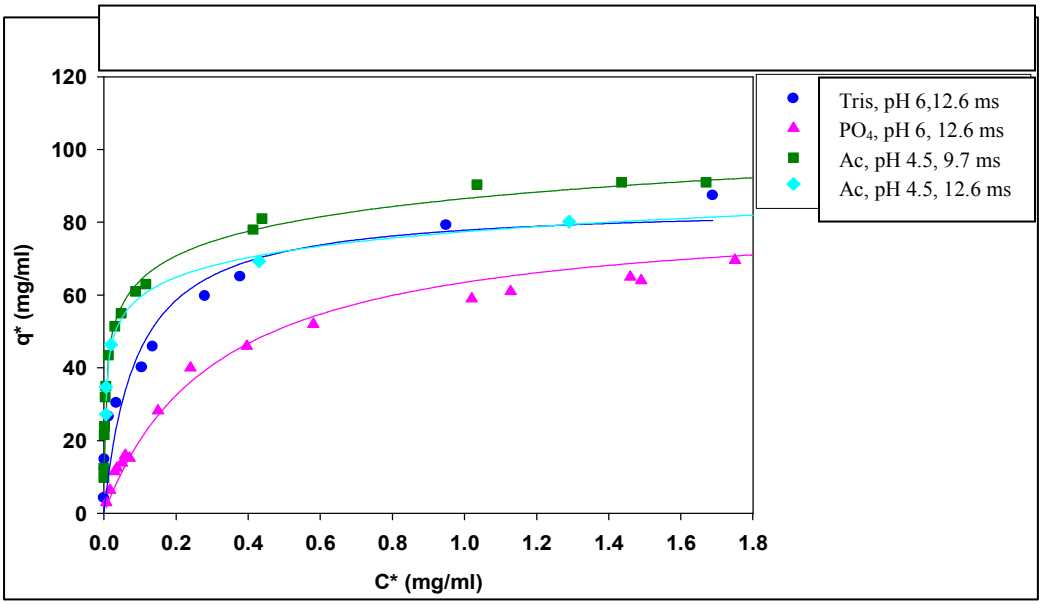

Figure 2.1 Lysozyme equilibrium binding curves in 50 mM Tris (pH 6), and 50 mM sodium phosphate (pH 6) and 50 mM Acetate (pH 4.5). (Trend lines represent Langmuir model)

Table 2.2 Langmuir parameters of HEWLZ determined for equilibrium concentration range 0-1.8 mg/ml.

Buffer	pH	Conductivity(mS)	K_d (mg/ml)	q_m (mg/ml)
Sodium acetate	4.5	9.7	0.008 ± 0.0045	94 ± 4.0
Sodium acetate	4.5	12.6	0.011 ± 0.0023	81 ± 3.8
Sodium phosphate	6.0	12.6	0.23 ± 0.016	74 ± 1.5
Tris	6.0	12.6	0.09 ± 0.03	84 ± 5.0

Lysozyme adsorption at pH 4.5 in 50 mM sodium acetate and 50 mM NaCl had an ionic strength of 0.1 (Equation 3) and conductivity of 9.7 mS. To compare pHs at similar conductivities another pH 4.5 solution was prepared, where conductivity was adjusted to 12.6 mS by using 73 mM NaCl in 50 mM sodium acetate buffer. Comparison of pH 4.5

and 6.0 are seen in Figure 2.1. At pH 4.5 and conductivity of 9.7 mS lysozyme adsorption reached 94 mg/ml level and at 12.6 mS a slightly lower value of 81 mg/ml. At pH 6.0 and conductivity of 12.6 mS, lysozyme adsorption in phosphate buffer reached 74 mg/ml and 84 mg/ml in Tris. Binding capacity was higher for pH 4.5 than either pH 6.0 buffer. This difference probably reflects greater charge density of HEWLZ at pH 4.5. From Figure 2.1 it seems that pH 4.5 at 12.6 mS and Tris at pH 6 have similar binding capacity of about 74 mg/ml, which can be explained by the final pH of the Tris- lysozyme of 5.1.

Lysozyme adsorption in pH 4.5 buffer at the same conductivity (12.6 mS) as both the pH 6 buffers has a higher binding capacity than pH 6 in sodium phosphate. Each set of the equilibrium data for Figure 2.1 was fitted to the Langmuir model by a non-linear least-square regression analysis to determine the parameters listed in Table 2.2. Standard error of each of these parameters was obtained using Sigma plot. The parameter q_m shows the maximum amount of lysozyme bound to the cation exchanger; K_d is a measure of strength stability of the complex formed between the protein and the exchanger under specific experimental conditions. For example, a large K_d value indicates that the protein has a low binding affinity for the exchanger.

The parameters listed in Table 2.2 show that there is a decrease in maximum binding capacity and increase in the dissociation constant with an increase in pH. Both Tris buffer and sodium phosphate increased maximum binding and decreased dissociation constant significantly. Binding of lysozyme to SP Sepharose dropped by 9% and binding strength decreased by 21% in phosphate buffer as the pH was raised from 4.5 to 6.0. This kind of binding pattern suggests that changes in the degree of ionization of basic groups on lysozyme, i.e. the histidine, lysine and arginine side chains are very small in the higher pH range (*28*).

2.3.2 Effect of phytic acid on lysozyme adsorption

To assess the effect of phytic acid on lysozyme adsorption to the cation-exchange resin, adsorption isotherms as a function of different buffers ions and pH were generated. HEWLZ adsorption from pH 6.0 phosphate buffer with and without phytic acid were performed in 50 mM sodium phosphate buffer and 50mM NaCl. The conductivity of the lysozyme in 50 mM phosphate buffer containing phytic acid varied from 12.6 to 14.7 mS (due to contributing from sodium phytate). HEWLZ adsorptions from pH 6.0 Tris buffer with and without phytic acid were performed in 50 mM Tris buffer and 73 mM NaCl. The conductivity of the lysozyme in 50mM Tris buffer containing phytic acid varied from 12.6 to 14.0 mS. The pH 4.5 adsorption of HEWLZ with and without phytic acid was performed in 50 mM sodium acetate and 50 mM NaCl. The conductivity of the lysozyme in acetate buffer containing phytic acid varied from 9.2 to 11.3mS.

The equilibrium adsorption isotherms of lysozyme on SP Sepharose with and without phytic acid added are shown on Figure 2.2. The effects of phytic acid on binding capacity and affinity for different conditions were similar to those that were mostly used in HEWLZ extraction and purification processes in earlier studies (*2*). The overall binding capacity and strength decreased with phytic acid addition to HEWLZ solutions (Tables 2.3 and 2.4). At pH 4.5, maximum adsorbed lysozyme decreased from 94 to 58 mg/ml resin (Table 2.4). Similarly, the maximum binding capacity in 50 mM phosphate buffer, pH 6, decreased from 74 to 56.6 mg/ml. On the other hand in 50 mM Tris buffer of pH 6, the binding decrease from 84 to 63 mg/ml. The effect of phytic acid on lysozyme adsorption was more pronounced at pH 4.5 than pH 6.0. In the presence of phytic acid the maximum lysozyme adsorption differed by 40% at pH 4.5 while only 24% at pH 6.0 in phosphate buffer. In case of phosphate and Tris buffers, effect of phytic acid on HEWLZ adsorption capacity was similar. In Tris buffer of pH 6.0, maximum adsorption differed by 25% when phytic acid added.

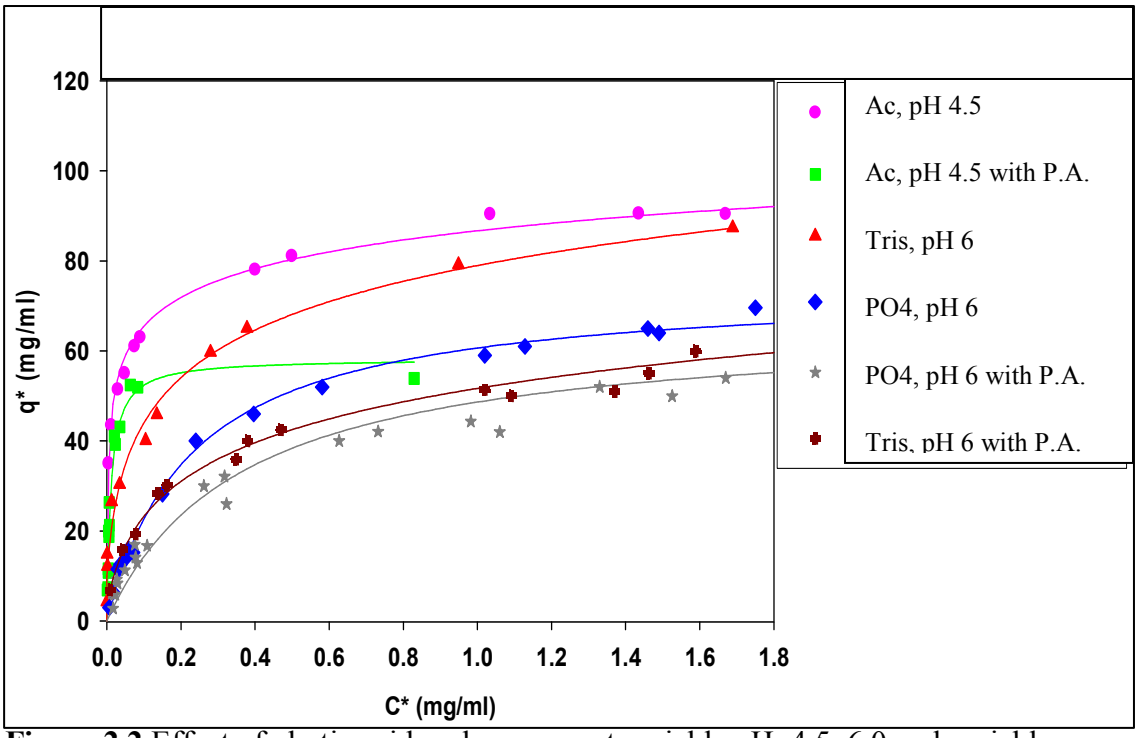

Figure 2.2 Effect of phytic acid on lysozyme at variable pH; 4.5, 6.0 and variable buffers; 50 mM sodium phosphate, 50 mM Tris. [a]P.A.= phytic acid (Trend lines represent Langmuir model)

Table 2.3 Effect of phytic acid on dissociation constant, K_d in 0 - 1.8 mg/ml supernatant concentration range. (*NaAc concentration exception)

Buffer	**pH & Conductivity**	**K_d (mg/ml)**	**K_d w Phytic acid (mg/ml)**	**Conductivity w Phytic Acid (mS)**
Sodium Acetate	4.5 9.7mS	0.008 ± 0.0045	0.013 ± 0.0015 (0-0.83mg/ml)	9.2 -11.3
Sodium Phosphate	6.0 12.6mS	0.23 ± 0.016	0.30 ± 0.03	12.6 -14.7
Tris Buffer	6.0 12.6mS	0.09 ± 0.03	0.20± 0.036	12.6 – 14

Table 2.4 Effect of phytic acid on maximum binding capacity, q_m in 0-1.8 mg/ml supernatant concentration range.

Buffer	**pH & Conductivity**	**q_m (mg/ml)**	**q_m w Phytic Acid (mg/ml)**	**Conductivity w Phytic Acid (mS)**
Sodium Acetate	4.5 9.7mS	94 ± 4	58.3 ± 2.4 (0-0.83mg/ml)	9.2 -11.3
Sodium Phosphate	6.0 12.6mS	74 ± 1.5	56.6 ± 2	12.6 -14.7
Tris Buffer	6.0 12.6mS	84 ± 5	63 ± 2.9	12.6 – 14

At pH 4.5, HEWLZ formed a white precipitate when phytic acid was added to solutions containing more than 3.6 mg/ml of lysozyme. Because of the precipitate formation, equilibrium adsorption of lysozyme with phytic acid at pH 4.5 could not be carried out at initial concentrations greater than 2.5 mg/ml (Figure 2.3). To examine the effect of conductivity variation on adsorption parameters, the experimental data for the HEWLZ concentration range of 0 to 0.1 mg/ml was re-plotted in Figure 2.3. In this protein concentrating range here was only a slight variation in conductivity (12.6 to 13.07 mS). The equivalent initial concentration, Co and its conductivity to the equilibrium concentration shown in Figures 2.2 and 2.3 can be found in the appendix.

Tables 2.3 and 2.4 shows the calculated dissociation constant and maximum binding capacity, respectively, with individual standard error for the different pH's and buffers within the supernatant concentration range of 0 through 1.8 mg/ml. The only exception is the parameters for pH 4.5 with phytic acid. In this case, 0.83 mg/ml is the highest equilibrium concentration the experiment is performed up to that equals to an initial concentration of 3.6 mg/ml. Any concentration higher than 3.6 mg/ml tends to precipitate. From the data, phytic acid decreases the maximum binding capacities and increases the dissociation constants significantly for pH 4.5 and pH 6 in Tris and phosphate to some extent.

In the lower HEWLZ concentration range of 0 through 0.6 mg/ml, adsorption values at pH 4.5 were higher than those for Tris and sodium phosphate buffer pH 6 (Figure 2.3) . This is consistent with the estimated K_d values in Table 2.1. Even though HEWLZ in pH 6 Tris buffer showed almost similar maximum binding capacity, q_m as pH 4.5 with 12.6mS, the binding affinity, K_d was larger for pH 6 in Tris buffer since the binding strength was stronger at pH 4.5 than pH 6.0. Therefore, the overall binding affinity for HEWLZ in pH 6 Tris buffer was not as strong as pH 4.5 and the K_d was still large compared to the K_d for pH 4.5.

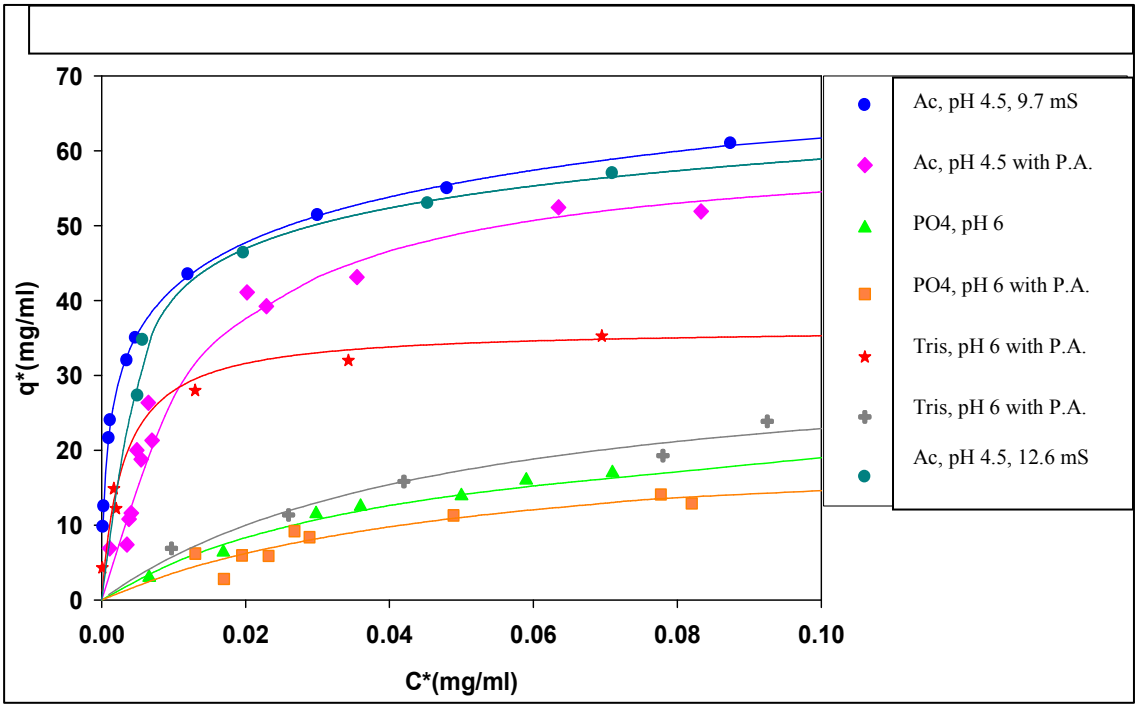

Figure 2.3 Effect of phytic acid on lysozyme at variable pH; 4.5, 6.0 and variable buffers; 50 mM sodium phosphate, 50 mM Tris at very low concentrations (0-0.1 mg/ml).
[a]P.A. =phytic acid

Binding strength decreased by 62% for pH 4.5, 30.4% for pH 6.0 in phosphate, and >100% for pH 6.0 in Tris when phytic acid was added to lysozyme during the adsorption study. The results for pH 6.0 in Tris had uncertainty because later it was discovered that the pH consistency was a problem when tris buffer used both for pure lysozyme and lysozyme with phytic acid solution (0 to 1.8 mg/ml). However, at lower concentration range of 0-0.1 mg/ml of equilibrium concentration, C* which are equivalent to 0.4-1 mg/ml of initial concentration, C_o, pH change was not significant. Yet there was

significant difference between pure lysozyme and lysozyme with phytic acid adsorption on the ion exchanger shown on Figure 2.3. Therefore, effect of phytic acid on lysozyme adsorption on SP Sepharose seems to be considerable.

It is reasonable to assume that phytic acid has an effect on lysozyme adsorption mainly because of two reasons regardless of any pH inconsistencies at high concentrations of lysozyme and phytic acid solution; First at very low initial concentrations of lysozyme and phytic acid (0 to 3.6 mg/ml) the pH of the solution was not affected but in Figure 2.3 the difference in lysozyme adsorption on the cation-exchanger is seen clearly when phytic acid added. Second when pH adjustment tests from 4.5 to 6.0 were done (Figure 2.4) during the uptake of protein, there was significant difference between pure lysozyme and lysozyme with phytic acid uptake in the cation-exchanger even though the pH consistency was maintained during the uptake.

Table 2.5 Effect of phytic acid on dissociation constant, K_d, at low (0 -0.1 mg/ml) equilibrium concentration range.

Buffer	**pH & Conductivity**	**K_d (mg/ml)**	**K_d with Phytic acid (mg/ml)**	**Conductivity with Phytic Acid (mS)**
Sodium Acetate	4.5 9.7mS	0.002 ± 0.0004	0.013 ± 0.0015	9.2 -10.96
Sodium Phosphate	6.0 12.6mS	0.04 ± 0.012	0.09 ± 0.02	12.6 -13.09
Tris Buffer	6.0 12.6mS	0.006 ± 0.0012	0.07 ± 0.017	12.6 – 12.7

Table 2.6 Effect of phytic acid on binding capacity, q_m at low (0 -0.1 mg/ml) equilibrium concentration range.

Buffer	**pH & Conductivity**	**q_m (mg/ml)**	**q_m w Phytic Acid (mg/ml)**	**Conductivity with Phytic Acid (mS)**
Sodium Acetate	4.5 9.7mS	60 ± 2	50 ± 3	9.2 -10.96
Sodium Phosphate	6.0 12.6mS	30 ± 3.5	18 ± 4.85	12.6 -13.09
Tris Buffer	6.0 12.6mS	42 ± 2.9	25 ± 5	12.6 – 12.7

Tables 2.5 and 2.6 above shows the effect of phytic acid on dissociation constant and maximum binding capacity for pH 4.5 and 6.0 and equilibrium concentrations of 0 through 0.1 mg/ml. At lower concentration range, pH and conductivity change was not significant. Therefore, the effect of phytic acid on lysozyme adsorption was better seen. Both the pH and conductivities were not significantly different when phytic acid was added to lysozyme. In the lower concentration range, maximum binding capacity of lysozyme decreased by 17% at pH 4.5, 40% in the phosphate buffer, pH 6 and 40% in tris buffer, pH 6.0. Binding strength of lysozyme was significantly lower when phytic acid was added as the K_d increased in all the cases. Therefore, the phytic acid effect on HEWLZ interaction with the cation exchange resin was easier to discern in the lower concentration range.

2.3.3 Comment on the effect of phytic acid on buffer pH

Comparing Tris and phosphate buffers of pH 6.0, it was observed that Tris displayed a greater variation in pH when phytic acid added (Table 2.7) It was difficult to maintain a constant pH when Tris buffer was used. There was an increase in pH with an increase in lysozyme and phytic acid concentration and a decrease in pH with just pure lysozyme solution in Tris buffer. Using phosphate or acetate buffers, pH was not affected in the pure lysozyme solution but was slightly affected when phytic acid was added.

Table 2.7 Summary of pH changes at high concentrations of lysozyme with phytic acid.

pH	Co(mg/ml)	Buffer	Protein	Phytic acid	pH Change
4.5	5	Acetate	Yes	None	None
4.5	3.5	Acetate	Yes	Yes	+ 0.5
6	5	PO4	Yes	None	None
6	5	PO4	Yes	Yes	+ 0.5
6	4	PO4	Yes	Yes	+ 0.4
6	2	PO4	Yes	Yes	+ 0.2
6	4.8	Tris	Yes	None	- 0.9
6	4.8	Tris	Yes	Yes	+ 1.8

[a]molar ratio of lysozyme (LZ) to phytic acid is 1:10, C_o=initial concentration

There may be several factors influencing the results of phytic acid effect on different pH and buffers. Both net charge and distribution of charges on HEWLZ changes differently when phytic acid was added at the two pH's. The number of charges on a protein at a particular pH can be calculated if the pK_a values of all the ionizable groups are known. For lysozyme the numbers of such groups and their pK_a values have been determined (*73*). At pH 5, the number of positive and negative charges of HEWLZ is calculated to be 19 and 8 respectively (*28, 73*). Therefore, at pH 4.5 HEWLZ is not only more positively charged, it would also have an asymmetric distribution of negative charges. Negatively charged phytic acid interaction with such a state of charge distribution on the surface of protein may change the energetically equivalent contact area that interact with exchanger sites. Since the ratio of positive to negative charge should have a smaller difference in the HEWLZ solution containing phytic acid than a pure HEWLZ solution, this may change/decrease the average no. of binding between HEWLZ and SP Sepharose. In case of pH 6.0 similar things happen but even a smaller difference is expected.

2.3.4 Phytic acid effect on HEWLZ uptake

Pure protein and lysozyme with phytic acid uptakes were performed to investigate if phytic acid effect was evident during the initial 5 minutes of the protein uptake experiments. The results for the 6 uptake experiments shown on Figure 2.4 correlate well with equilibrium adsorption data. Since all the uptakes were started with an initial concentration below 2.0 mg/ml, pH and conductivity variation were not a concern.

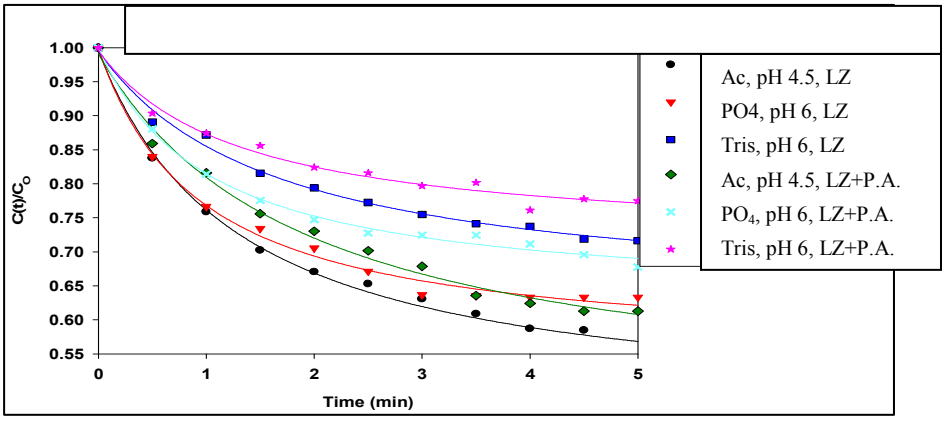

Figure 2.4 Protein uptake curves for HWELZ; effect of pH, buffer ion and of phytic acid. (The initial HEWLZ concentration was 2 mg/ml) [a]P.A.=phytic acid, LZ=lysozyme

The initial slopes of uptake curves in Figure 2.4 suggest that the rate of uptake of lysozyme in each buffer decreased in the presence of phytic acid. The HEWLZ uptake rate in Tris buffer was apparently lower compared with pH 4.5 acetate and pH 6.0 phosphate buffer Each buffer pair (pure lysozyme versus lysozyme and phytic acid) shows a difference in the uptake rate. When phytic acid was added to pure lysozyme, the rate of uptake (initial slope) decreased by 15% for pH 4.5 in acetate, 13.5% for pH 6.0 in phosphate and 15% for pH 6.0 in Tris buffer. The difference between the amount of HEWLZ uptake after 5 min and equilibrium values were 90% for pure lysozyme at pH 4.5, 88% for pure lysozyme at pH 6.0 phosphate buffer and, 75% for pure lysozyme in Tris. In the experiments with HEWLZ and phytic acid mixtures, the difference between uptake and equilibrium binding values was 84% at pH 4.5, 85% in pH 6.0 phosphate and 88% in pH 6.0 in Tris buffer.

2.3.5 Effect of pH 4.5 to pH 6 adjustment on HEWLZ uptake

In the previous studies, the adjustment of pH 4.5 extract to pH 6.0 resulted in a significant decrease (8 to 30-40 mg/ml) in HEWLZ binding capacity to SP Sepharose. Therefore, pH 4.5 to 6.0 adjustment tests were performed to understand whether phytic acid caused the drastic reduction in binding capacity. pH of HEWLZ solutions (2 mg/ml) prepared in acetate buffer was adjusted using sodium hydroxide (0.5M), phosphate (1M), and Tris (1M). Phytic acid was added to the pH adjusted HEWLZ solution and lysozyme uptake was observed over a period of 25 minutes.

Figure 2.5 shows a comparison of all the pH adjustment experiments. The highest rate of protein uptake was observed when pH was adjusted using phosphate buffer followed by sodium hydroxide and Tris. The trend lines of HEWLZ and phytic almost overlapped Figure 2.5. But, a significant difference of the uptake rates was seen between the pure lysozyme and lysozyme in the presence of phytic acid. When phytic acid was added, the initial rate of uptake decreased by 33% for NaOH pH adjustment with 0.5 M NaOH, 39% for 1 M phosphate adjustment and 33% for 1M Tris. Thus, the pH adjustment can be

done by either buffer or NaOH because there was no difference in the rate of uptake. On the other hand, pure lysozyme solutions were affected by the pH adjustment methods

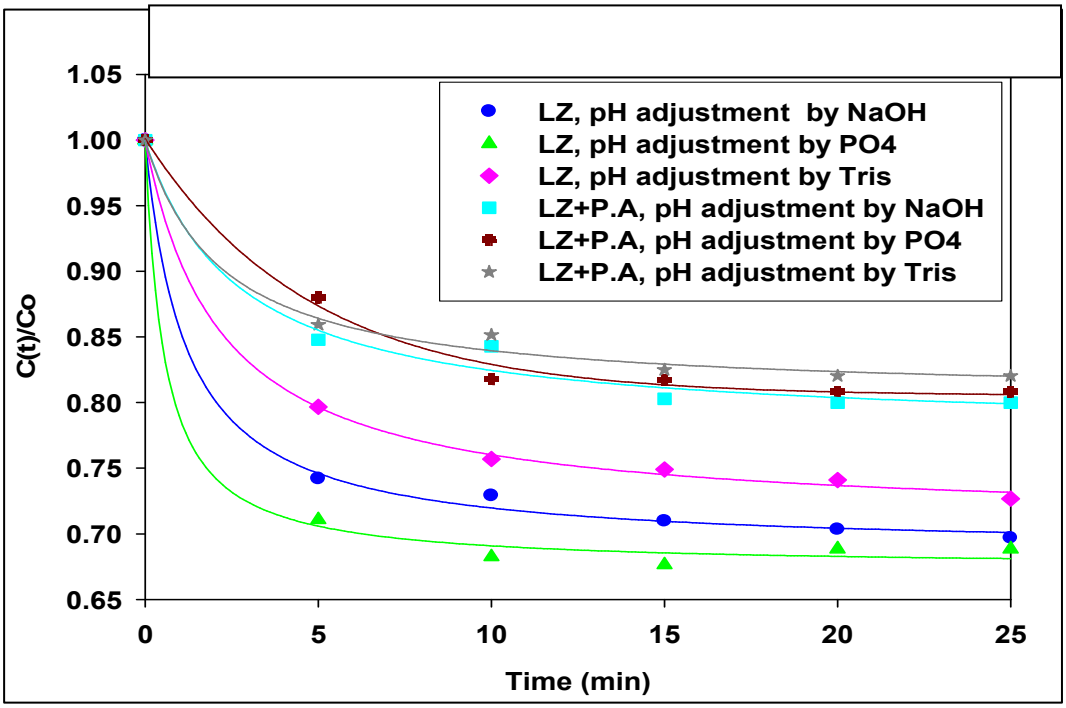

Figure 2.5 Protein uptake results showing the effect of phytic acid on lysozyme adsorption when pH was adjusted by using NaOH, PO4 and Tris. (Initial HEWLZ concentration was 2 mg/ml) [a]P.A.=phytic acid

2.4 Conclusion

This study demonstrated that lysozyme adsorption on SP Sepharose was affected by pH, buffer and a rice extract impurity, phytic acid. At constant ionic strength (conductivity), HEWLZ in pH 4.5 acetate buffer had a higher binding capacity and stronger binding strength than at pH 6.0. HEWLZ in sodium phosphate buffer, pH 6.0, exhibited lower adsorption of lysozyme than in pH 6 Tris buffer. Binding capacity and strength were significantly affected by phytic acid in all buffers. Therefore, removing phytic acid from rice extract could increase lysozyme binding capacity from 17% to 40% at pH 4.5, from 24% to 40% in phosphate and from 25% to 40% in Tris buffer. Langmuir model was a useful tool in comparing the optimum conditions for lysozyme adsorption and determining the effect of phytic acid on lysozyme adsorption on SP Sepharose.

CHAPTER III

MODIFICATION OF MICROFILTRATION MEMBRANE SURFACES TO REDUCE FOULING

3.1 Introduction

Microfiltration (MF) in protein purification is an emerging unit operation in the biotechnological industries that is expected to lower downstream processing cost and achieve higher throughputs (*34-44*). Microfiltration membranes involved in separation and purification of proteins from complex mixtures have a typical pore diameter in the range of 0.1 – 0.6 μm (*45, 48*). MF membranes are made from natural or synthetic polymers such as cellulose acetate, polyvinylidene difluoride (PVDF), polyamides, polysulfone, polypropylene, and PTFE and inorganic materials such as metal oxides (alumina), glass, and zirconia coated carbon. Typical uses of microfiltration with ceramic membranes include primary cell recovery from fermentation broths, sterile filtration (*46*), preparation of parenterals and sterile water for pharmaceutical industry (*47*), concentration of fruit juices and alcoholic beverages (*32, 33*), waste treatment for removing intractable particles in oily fluids (*32*).

Membrane fouling is a major impediment to using MF for protein purification. Fouling is caused by protein adsorption to the membrane surface including pore. Membrane surface chemistry, protein structure, magnitude and charge of both the protein and membrane surface and the degree of hydration of the protein are all important factors in determining fouling (*46*). Membrane fouling causes a loss of membrane permeability that occurs over time and results from an accumulation of material called foulant on the surface and within the porous structure of the membrane during filtration (*56, 57*). There is usually a monolayer or multilayer of macromolecules adsorbed on the membrane surface and on the walls of membrane pores during membrane fouling. The tightly bound adsorbed monolayer that cannot be removed by rinsing with water and requires application of chemical treatments is known as irreversible fouling (*58*). Deposition of denatured and aggregated macromolecules and other feed stream components on the monolayer (*58*) that can be removed by cleaning with water is referred to as reversible fouling (*58, 59*).

Fouling by proteins involves interaction with membrane surface through electrostatic attraction, hydrogen bonding and van der Waals and dispersion forces (*48*). Modification of membrane surface is a plausible approach reducing fouling of membrane surfaces. Several publications have shown polyethylene glycol (PEG) reduces protein adsorption because of its hydrophylic nature, steric repulsion and exclusion volume effect (*84-87*). Other studies have shown that cellulose and its derivatives such as cellulose esters foul less and have excellent mechanical strength (*89*). Cellulose-based membranes have disadvantages such as swelling in water and pore size change with temperature and pressure (*90*). From literature review, membrane usage for protein purification has been limited to polysufone materials because commercial alumina membranes (*91-93*) display drastic fouling. Therefore, it would be useful to design hybrid membranes that would consist of high pore size uniformity and potential diversity in surface chemistry. In this paper, two different proteins, bovine serum albumin (BSA) and immunoglobulin G (IgG), have been used to study fouling and interaction with bare alumina and modified alumina membrane surfaces.

IgG (MAbs) are the most important class of pharmaceutical proteins that are currently developed for therapeutic and diagnostic purposes. IgG molecules has extraordinary specificity and binding affinity for immobilized protein A that is a basis of various types of immunoassays (*48, 74*). Protein A is a cell wall component of *Staphylococcus aureas* that has a cell wall/membrane associated region consisting of a linear series of 5 highly homologous antibody binding domains (*68*). At Lowe's lab (*70*), Lowe and collaborators developed protein A mimetic ligand that was attached to MF membrane in such a way across the tubular membrane while the remainder of the mixture did not cross the membrane and selectively binded IgG to the functionalized nanoparticles. This paper is focused on fouling and the adsorption of native human IgG to various membranes and to protein A mimetic ligand membrane to compare the specificity of the latter membrane to others. In preparation of the membranes used for fouling study in this paper, the membranes were modified to acquire functional groups to reduce fouling or selectively bind IgG. According to Zeng and Ruckenstein (*48*) an ideal membrane should have a microporous or macroporous structure for rapid flow, available reactive groups for

coupling of functional ligands, chemical and physical stability to tolerate harsh operating and/or cleaning conditions and a hydrophilic surface for prevention of nonspecific binding.

3.2 Experimental

3.2.1 Material

The model protein, bovine serum albumin (BSA, Aldrich (A7906), MW 67kD, pI 4.7) and immunoglobulin G (IgG, Sigma Chemical Co. MW 16 kD, pI 8.3) were used as model proteins to investigate the membrane fouling behavior and used for protein analysis and quantification. Anopore alumina membranes (Whatman, 25 mm diameter membranes, 200 nm diameter cylindrical macropores, used as received) were used as the adsorbent media for the protein. Materials used for functionalization of the membranes were tetraethylorthosilicate, TEOS 99%, (Fluka), 3-aminopropyltriethoxysilane, APTES 99%, piperazine 99%, N,N-diisopropylethylamine, 99% (Aldrich), Cyanuric chloride, CC 99% (ACROS), Succinimidyl ester of methoxy poly (ethylene glycol) propionic acid, mPEG-SPA, 5kDa (Nektar), ethanol, and dichloromethane, DCM, ACS reagent grade (EMD). Materials used for equilibration buffer, phosphate buffered saline (PBS), preparation were sodium phosphate, dibasic, 12-hydrate, crystal (J.T. Baker L#Y49582), sodium hydroxide (Fisher Scientific), and potassium phosphate monobasic (J.T.Baker). Membrane cleaning solutions were tetrahydrofuran (THF), methanol, toluene, both ACS reagent grade (Aldrich) and RO water.

3.2.2 Analytical methods

Analytical balance of 0.001g reliability was used to weigh out the protein powder. DU 640 UV Spectrophotometer, (Beckman Coulter) was used to determine protein concentration before and after adsorption. For determining low protein concentrations outside the 280 nm absorbance r range, Bradford method (*11*) with bovine serum albumin as a standard was used. Water permeation experiments were performed in a 25 mm diameter stirred cell (Model 8010, Amicon) connected to a N_2 pressurized solution

reservoir at room temperature. A digital timer was used to measure the flow of water through the membranes during the water permeation tests. The protein profiles during the desorption study and fractions were evaluated by gel electrophoresis (*40*). Samples were analyzed on 8-16% tris-glycine gels under nonreducing conditions.

3.2.3 Membrane synthesis

Membranes used to study fouling were alumina (bare) membrane, silica-coated membrane, amine -unctionalized membrane, and polyethylene glycol (PEG) – functionalized membrane. Protein A mimetic membranes were prepared to selectively attaching protein A mimetic ligand to amine-functionalized membranes via triazine.

3.2.3.1 Preparation of silica-coated membrane. Anopore alumina membrane was coated with a silica layer by immersing the membrane in a solution containing 100 mg of TEOS with 50 mL of ethanol (10 mM) that contains 1.3 mL of HCl (0.032 N) at room temperature for 2 h. After this silica layer had been deposited on the alumina membrane surface, the membrane was removed from this coating solution and dried at 95 °C for 15 min. The membrane was then cooled to room temperature and was ready to use for protein adsorption experiments.

3.2.3.2 Preparation of amine-functionalized membrane. Synthesis of amine-functionalized membrane was started with the silica coated membrane. After the silica layer was deposited as mentioned above (3.3.1), the silica coated membrane was immersed into a solution of 440 mg of APTES in 200 mL toluene (10 mM) at room temperature for 24 h. Silica coating was important prior to amine functionalization due to difficulty of achieving high graft densities on alumina surfaces using just the amine synthesis approach as shown in previous studies (*36, 38*). After the 24 hr period, the membrane was removed from the solution and repeatedly rinsed with toluene, THF, methanol and water to remove excess APTES. The amine functionalized membranes were then dried for 30 min at room temperature and further used for adsorption experiments.

3.2.3.3 Preparation of PEG-functionalized membrane. For preparing PEG-functionalized membranes amine functionalized membrane was immersed into a solution of 1.4 g of cyanuric chloride (CC) in 50 mL of THF (0.15M) with 1 mL of DIPEA. This solution with the membrane was then slowly rocked at about 30 rpm on a shaker plate at room temperature for 10 h. After the membrane was treated in that solution it was rinsed three times in 20 ml of THF for 10 to 15 minutes followed by two times 20 ml rinsing methanol, two times 20 ml in DCM, and two times 20 ml in THF. After the rinsing was completed the membrane was immersed in a solution of 1.3 g of piperazine in 50 mL (0.3 M) of THF and heated to 60 °C for 14 h. After the 14 hr period, this membrane was rinsed 10 to 15 min three times with 20 ml of THF, two times with 20 ml of methanol, two times with 20 ml of DCM, and two times with 20 ml of THF. The final THF rinse in both steps was checked by TLC (Thin Layer Chromatography) for trace amounts of triazine and amine. Finally, mPEG-SPA covalent attachment was performed to the melamine based synthesized membrane. This was done by subsequently immersing the synthesized membranes in a PEG solution containing 500 mg of mPEG-SPA in 50 mL of water (2 mM)) for 2 h to react with mPEG-SPA. The PEG synthesized membranes were then used for adsorption experiments.

3.2.3.4 Preparation of protein A-mimetic ligand membranes. Amine functionalized membrane was used to synthesize the protein A mimetic ligand membranes. Cyanuric chloride was attached to the amine-functionalized membrane by immersing the membrane into a solution of 1.4 g of cyanuric chloride (CC) in 50 ml of THF (0.15M) with 1 ml of DIPEA. A 1.2 eqivalent aniline solution (22.4 mg of aniline in 50 ml THF + 0.105 ml of DIPEA (diisopropylethylamine) for 24 h at room temperature was added that was based on the number of triazine groups on the surface. Cyanuric chloride functionalized membrane was added to 50 ml of THF and 3 equivalents of Hunigs base and reacted for 24 hours at RT. After that period, the membrane was rinsed with 50 ml portions of methanol, dichloromethane, and THF respectively. A solution containing 2 equivalents of tyramine (55 mg of tyramine in 50ml THF + 0.14 ml of DIPEA, diisopropylethylamine) based on the number of triazine groups in 50 ml of THF and 4

equivalents of Hunigs base was prepared. This solution was added to the membranes and heated at 50-60 ºC for 24 hours. After that period, the membrane was rinsed with 50 ml portions of methanol, dichloromethane, and THF respectively. Figure 3.1 shows the steps of the protein A mimetic ligand synthesis.

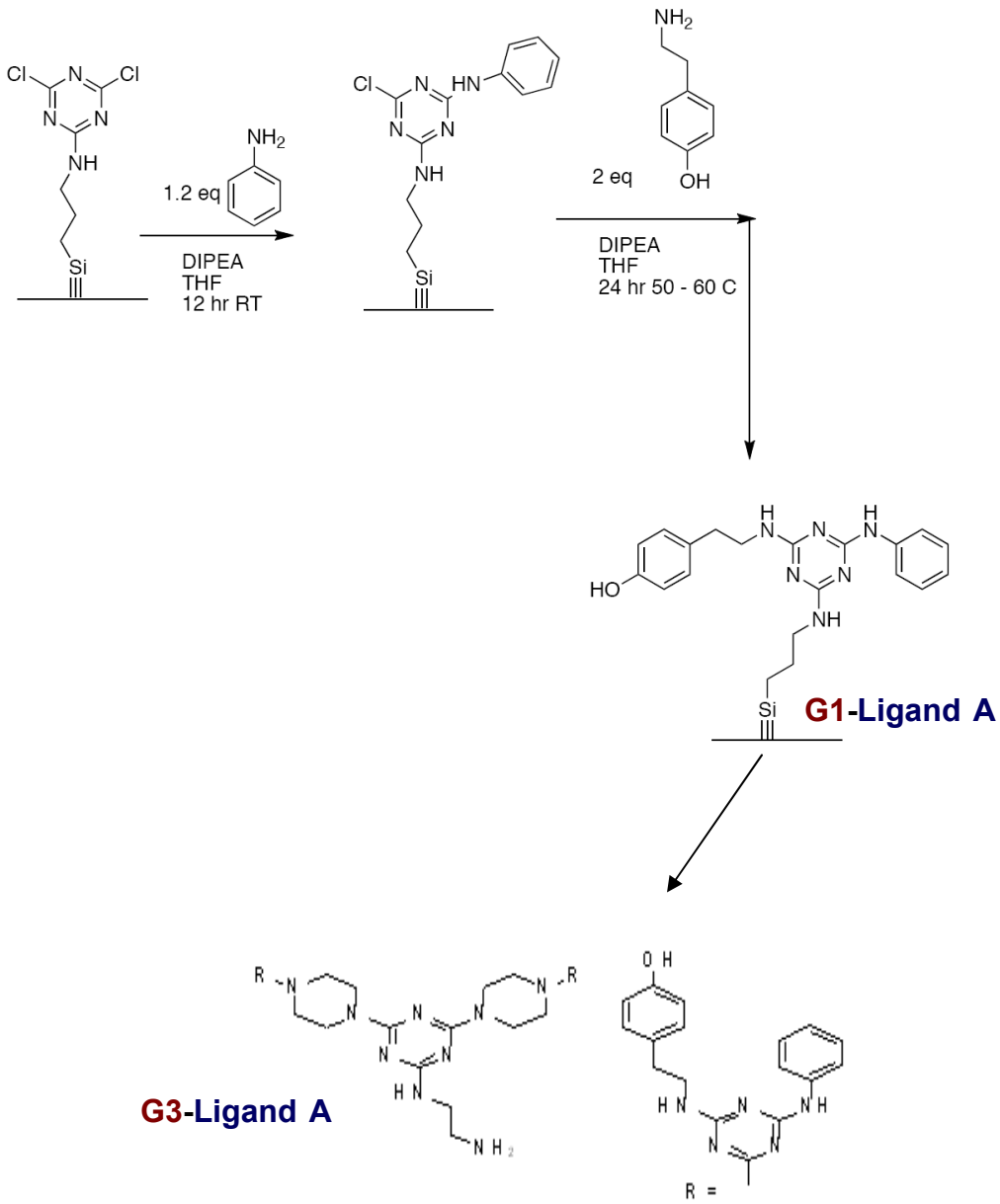

Figure 3.1 Synthesis of protein A mimetic ligand membrane to selectively bind IgG. (*70*)

G1, G2 and G3 membranes were designed to selectively bind IgG. G2 has double the number of IgG binding ligands (protein A mimetic ligand) compared to G1 followed by G3 that has double the amount of IgG binding ligands than in G2 membranes. Figure 3.1 shows the distribution of the protein A mimetic ligands on G3 membrane.

3.2.3.5 Adsorption isotherm experiment. Batch adsorption isotherms for BSA and IgG were developed by immersing a piece of membrane adsorbent (bare, silica-coated, amine - and PEG-functionalized) into 15 ml vial containing 10 ml of protein solution. Previously weighed protein was dissolved in adequate amount of the equilibration binding buffer, PBS at pH 7.4, to obtain the required initial protein concentration. The concentration of the prepared protein solution was then measured by absorption at 280 nm. An extinction coefficient of 0.667 ml/mg/cm (*33, 39*) for BSA and 1.40 ml/mg/cm for IgG was used (*39*). The protein concentration was varied from 0.3 to 2.7 mg/ml. Adsorption isotherms were generated over a period of 48 hrs at 4°C for all experiments. Incubation over a 3 day period gave similar results as 2-day incubation but resulted in higher BSA aggregation. One day incubation had almost half the protein adsorbed compared to the 2-day incubation.

Isotherms were developed under static condition at 4^{o}C because shaking the protein sample at room temperature resulted in aggregation of the protein. Potential aggregation was detected by measuring the absorbance of the protein solution at 420 nm. When the samples were incubated at 4°C protein (BSA) aggregation was negligible. At the end of the equilibration period, the supernatant protein concentration was measured by absorbance at 280 nm or using Bradford assay, if the concentration was below the detection limit. All protein solutions before and after the adsorption test were also checked for aggregation at 420 nm. The protein adsorbed (q*) at the end of the incubation time was calculated by Equation (3.1).

$$q^* = [(Co - C^*)^*V_{t]}/ A \qquad (3.1)$$

Where,

q*- the amount of protein adsorbed at equilibrium (mg/m^2)

Co - the concentration of initial protein solution (mg/ml)

C* - the amount of protein at equilibrium (mg/ml)

A - total surface area of the membrane (m^2)

Langmuir isotherm model was applied to fit experimental data and determine the maximum adsorption capacity (q_m) and dissociation constant (K_d).

$$q^* = q_m (C^*) / K_d + C^* \qquad (3.2)$$

Where,

q^* - protein adsorbed at equilibrium (mg/m^2)

q_m - maximum binding capacity (mg/m^2)

C* - supernatant concentration at equilibrium (mg/ml)

K_d - dissociation constant (mg/ml)

3.2.3.6 Water permeation test. All water permeation experiments were conducted after the 48 hrs of adsorption of BSA and IgG on to the different membranes. Water permeation was performed by flowing water through the fouled membrane in a 25 mm diameter stirred cell (Model 8010, Amicon) connected to a N_2 pressurized solution reservoir at room temperature. Figure 3.2 shows the experimental set up for the water permeation test. Pressure was varied from 1 psi to 15 psi. Initially water was flown at a constant pressure for about 2 minutes until steady state was achieved. Water flow was measured with change in pressure to determine the decline in flux and fouling during the water permeation test for the fouled membranes. A control for each type of membrane (non-fouled) was compared to the fouled membranes to show decrease in flux and permeability of the membranes.

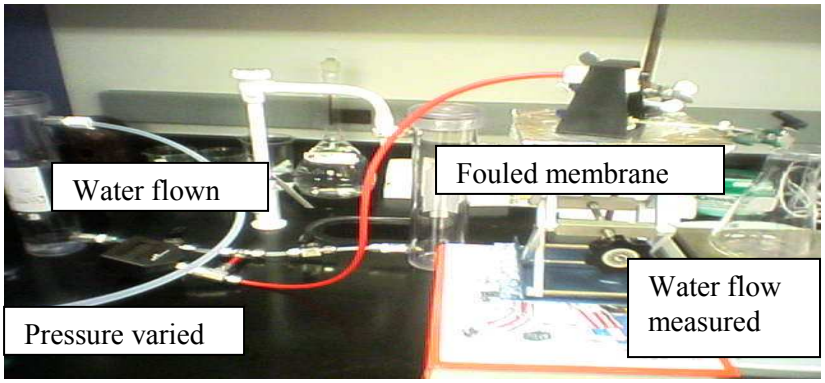

Figure 3.2 Water permeation experimental set up.

The water flux was determined by using Darcy's law to describe microfiltration as the flow through a porous medium (*44*). For a porous membrane, the permeate flux through the membrane, J ($m^3/m^2.s$), is given by equation 3.3. The permeate flux is proportional to the transmembrane pressure, ΔP (kPa) and inversely proportional to the membrane resistance, R (1/m) and the viscosity of the fluid, μ ($N.s/m^2$) (*49*):

$$J = Q/A = \Delta P/\mu.R \qquad (3.3)$$

Where,

Q - the permeate flow rate (m^3/s)

A - the membrane surface area (m^2)

ΔP - the transmembrane pressure (kPa)

μ - the fluid viscosity ($N.s/m^2$)

Further analysis can be done on the resistance, R in equation 3.4.

$$J = \Delta P /\mu (R_a+R_f+R_m) \qquad (3.4)$$

The resistance, R toward transport through the membrane can be divided in to membrane resistance (R_m), adsorption resistance (R_a) and fouling resistance (R_f). The membrane resistance is a membrane constant, adsorption resistance is used in evaluation of the static adsorption (concentration effect comes in to this term) and fouling resistance evaluates pressure forced adsorption (*50, 51*). Fouling resistance is thought of as a continuous growing cake on the membrane surface, where the first layer of the cake corresponds to the adsorbed monolayer (*50*). The cake resistance is a constant and is a function of the mass of permeate that passes the membrane (*50, 52*).

3.2.3.7 Desorption of IgG from protein A mimetic ligand membrane. Membranes with adsorbed IgG were treated with several buffer solutions and salt to determine level of desorption and assess the selectivity of protein A mimetic membranes. The protein adsorbed membrane was first placed in a vial containing 5 ml of PBS buffer to remove any non-specifically bound protein to the membrane surface. Each PBS buffer wash was about 15 min long, and was performed (about 4 times) until no protein was found in the washed solution. The concentration of the solution after the wash was measured by either

UV absorbance at 280 nm or using the Bradford assay. After the PBS wash, the membranes were washed once with 10 ml of 500 mM sodium chloride for about 30 minutes to remove any residual IgG protein adsorbed on the membrane. Finally, the membranes were immersed in 10 ml of 100 mM citrate buffer with a pH of 3.25 for about 30 min to specifically elute IgG attached to protein A mimetic ligand. The amount of desorbed protein was calculated from the amount of protein adsorbed on the membrane and the final protein concentration in the citrate wash. For the mixture of BSA and IgG, SDS-PAGE electrophoresis (*37*) was performed to monitor the removal of BSA and IgG during each desorption step. This sequence of washing steps was followed each time in order to regenerate the membranes after each adsorption cycle.

3.3 Results and Discussion

3.3.1 Protein adsorption on bare alumina membrane

The static adsorption measurement of bovine serum albumin (BSA) and immunoglobulin G (IgG) on alumina (bare) membrane is depicted in Figure 3.3. The initial concentration, C_o of BSA and IgG corresponding to the equilibrium concentrations, C*, shown in Figure 3.3 can be found in (the Appendix B). Since non-specific protein adsorption is considered as membrane fouling, the amount of maximum IgG adsorbed (22 mg/m^2) was higher on to the bare membranes compared to that of BSA (8.4 mg/m^2) (Figure 3.3). Amount of adsorbed protein was expressed per square meter of the membrane taking into account total membrane and pore surface areas. Adsorption of IgG was significantly higher than that of BSA on the bare membranes. In the lower initial concentration (about C_o=0.28 to 1.5 mg/ml), protein adsorption exhibited Langmuirian adsorption behavior. Martinez et al (*80*) showed that the higher concentration of γ-globulin fouling was fitted best a Freundlich heterogeneous isotherm, from which the pH dependence of active fouling sites and energies was obtained. Similarly, his initial concentration adsorption data obtained did not follow Langmuir behavior.

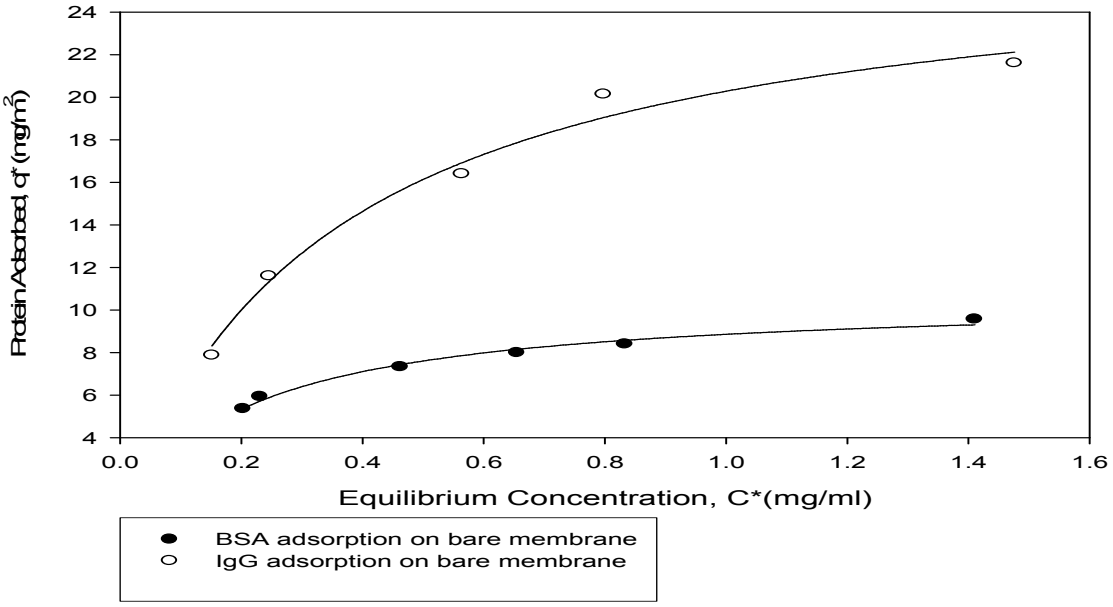

Figure 3.3 BSA and IgG adsorption isotherms on alumina (bare) membrane at pH 7.4 and 4 ºC and equilibrium concentration range of 0.2- 1.6 mg/ml.

Adsorption of proteins on alumina membrane can be explained by electrostatic interaction between the proteins and the membrane. The effective membrane charge of the alumina membrane at pH 7.4 determined from the number of ionizable groups resulted in negative effective membrane charge (*81*). Therefore, in the case of BSA and bare membrane, electrostatic repulsion during adsorption is expected because BSA is negatively charged at pH 7.4 (pI = 4.7) and membrane surface is also negatively charged at this pH. On the other hand, there should be electrostatic attraction between IgG and the bare membrane since IgG is positively charged at pH 7.4 (PI = 8.3). There may be higher non-specific adsorption in case of IgG than BSA.

3.3.2 Protein adsorption on silica-coated membranes

Silica-coated membrane showed similar adsorption characteristics as the bare membrane discussed in section 3.3.1. Figure 3.4 compares the adsorption of BSA and IgG on silica-coated membrane. Similar to the bare membrane, the amount of maximum IgG adsorbed (23 mg/m^2) was 3 times higher than that of BSA (7 mg/m^2).

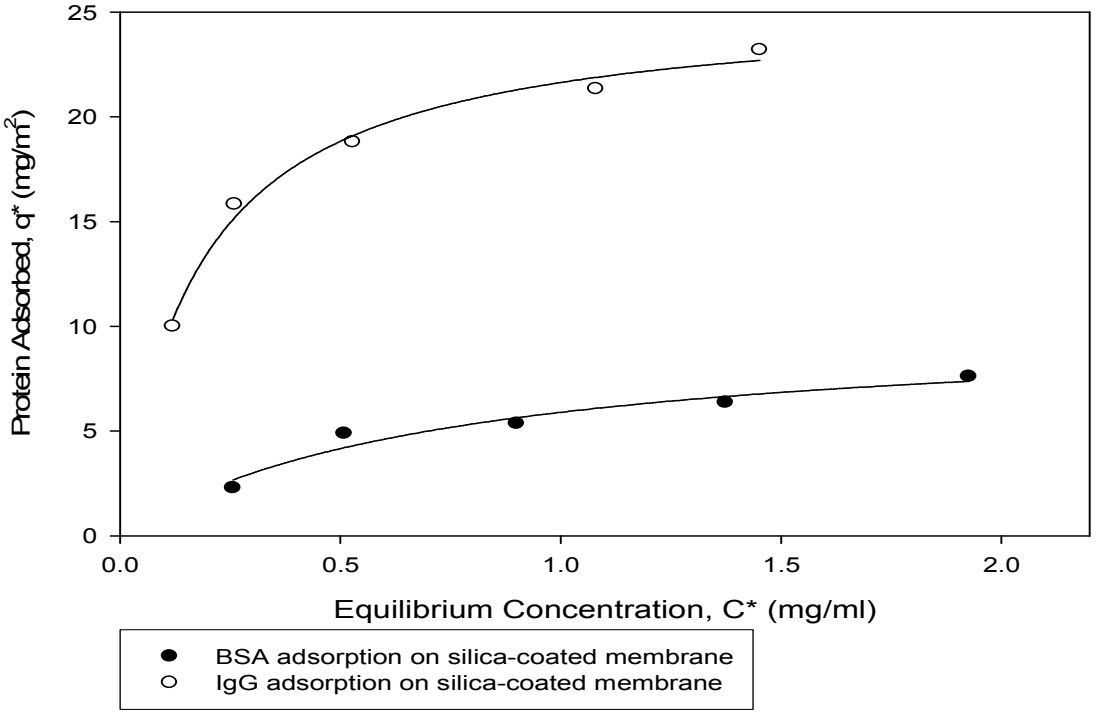

Figure 3.4 BSA and IgG adsorption isotherms on silica-coated membrane at pH 7.4 and 4 ºC and equilibrium concentration range of 0.2- 1.8 mg/ml.

Silica-coated membranes are more negatively charged at pH 7.4 compared to the bare alumina membranes because of the densely populated hydroxyl group on the silica surface (*82*). The adsorption of BSA and IgG on silica-coated membrane therefore followed a similar trend to that of bare membranes. BSA being negatively charged at pH 7.4 is probably electrostatically repulsed by the silica-coated membrane, and as a result, the adsorption of BSA on silica-coated membrane decreased by 12% compared to the bare membrane. This difference is based on the maximum adsorption. Contrary to BSA, , IgG adsorption on silica increased by 12% presumably due to stronger electrostatic attraction between positively charged IgG at pH 7.4 and more negatively charged silica-coated membrane.

3.3.3 Protein adsorption on amine-functionalized membrane

The static adsorption measurement of BSA and IgG on amine-functionalized membrane is depicted in Figure 3.5. The excess amine attachment to the silica surface gives the membrane a positive effective membrane charge.

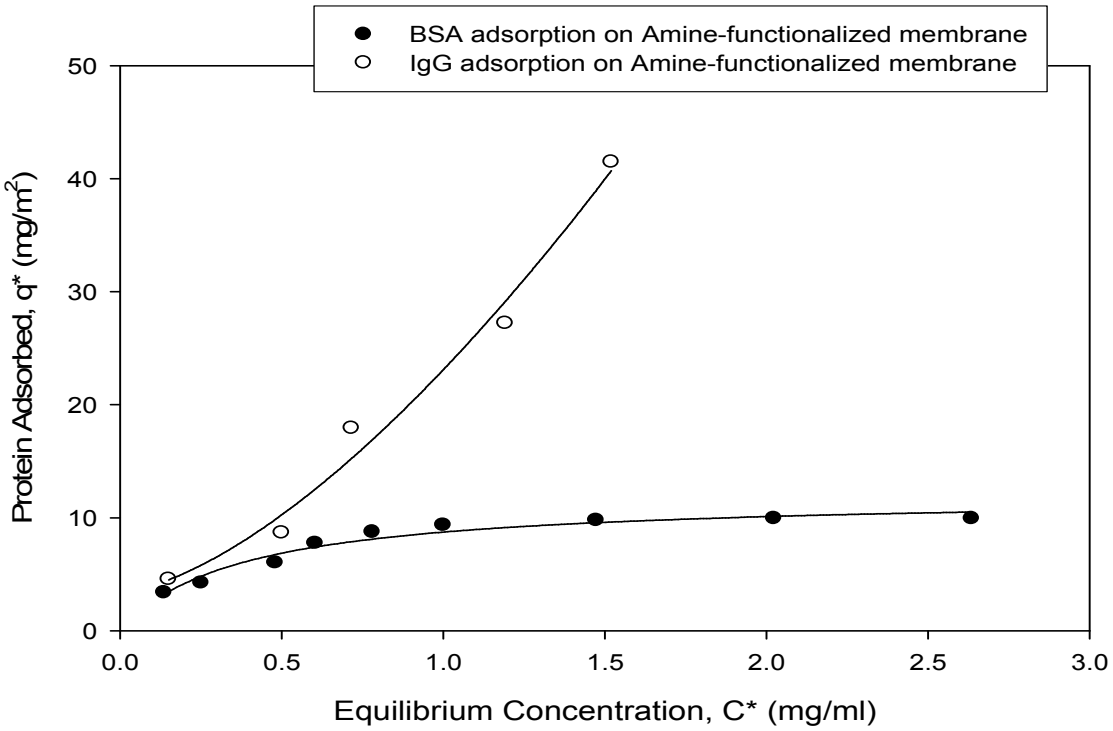

Figure 3.5 BSA and IgG adsorption isotherms on amine-functionalized membrane at pH 7.4 and 4 ºC and equilibrium concentration range of 0.2- 2.6 mg/ml.

Because amine-functionalized membranes are positively charged there is electrostatic attraction between BSA (negatively charged) at pH 7.4 and amine-functionalized membrane. Langmuir behavior of BSA adsorption to these membranes was observed, which suggests a specific adsorption of BSA on the amine-functionalized membrane (Figure 3.5). Maximum capacity of BSA adsorbed on amine-functionalized membrane was about 10 mg/m^2. This amount was 20% higher than the amount adsorbed on the bare membrane and 30% higher than the amount adsorbed on silica-coated membrane. This higher adsorption may be due to the electrostatic attraction between BSA and the amine functionalized membrane compared with the previous two modified membranes where electrostatic repulsion was presumably the dominating mechanism.

From Figure 3.5, IgG adsorption on amine-functionalized membrane did not follow Langmuir behavior. We hypothesize a multi-layers formation on the amine-functionalized membrane with IgG, because adsorption increased almost exponentially even at lower protein concentrations. Adsorption of IgG went up to 40 mg/m^2 on the amine-functionalized membrane at 1.5 mg/ml equilibrium concentration compared to 20 mg/m^2 (Figures 3.3 and 3.4) .

3.3.4 Protein adsorption on poly ethylene glycol (PEG) modified membrane

Figure 3.6 shows BSA adsorption on PEG-modified membranes, which followed Langmuirian behavior. BSA adsorption was the least on PEG –modified membranes.

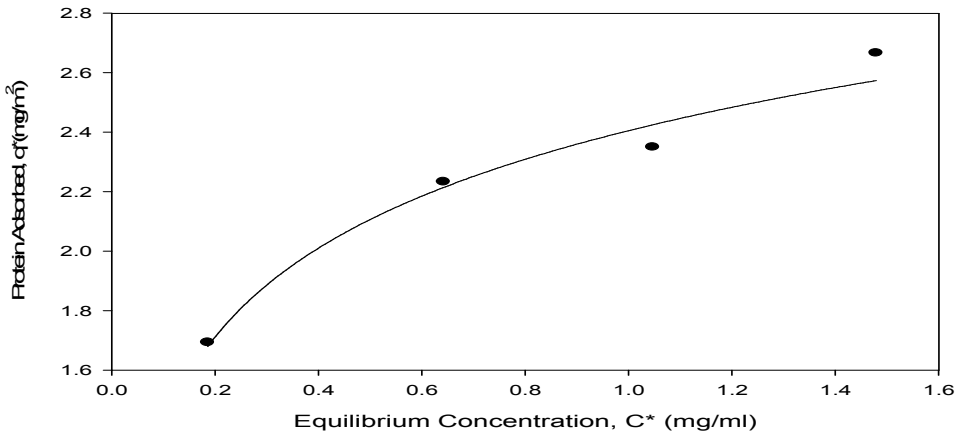

Figure 3.6 BSA adsorption isotherms on PEG functionalized membrane pH 7.4 and 4 ºC and equilibrium concentration range of 0.2- 1.6 mg/ml.

PEG membranes are hydrophilic in nature and have a steering effect on the surroundings because of its comb like structure on the membrane surface (*84-87*). Both these characteristics generally minimize protein adsorption on the PEG-modified membranes. IgG adsorption with PEG-modified membrane was not investigated.

The BSA adsorption data were fitted to the Langmuir model by a non-linear least-square regression analysis to determine the parameters listed in Table 3.1. Model parameters (q_m and K_d) were obtained from the data shown Figure 3.3 through 3.5. The parameter q_m shows the maximum amount of the protein bound to the membrane and K_d is a measure of the strength of interaction between the protein and membranes.

Table 3.1 Adsorption parameters for BSA and IgG on different membranes.

	BSA	BSA	IgG	IgG
Membrane	q_m	K_d	q_m	K_d
Bare	10.61± 0.28	0.19± 0.019	27.30±1.50	0.35±0.053
Silica coated	10 ± 1.37	0.48 ± 0.30	23.0± 1.35	0.71±0.24
Amine functionalized	12 ±0.60	0.25 ± 0.06	N/A Langmuir	N/A Langmuir

Langmuir parameters are consistent with the equilibrium adsorption data (Fig 3.3-3.5). Amine-functionalized membrane with BSA had the highest binding and a comparatively smaller dissociation constant, K_d, which represents strong binding. The q_m of bare membrane with BSA would be higher if more data points were taken into account. Since protein concentration range for the bare membrane (0.2 to 1.41 mg/ml) could fit the Langmuir model, the parameters were calculated based on that range. IgG on bare and silica-coated membranes gave similar results for maximum protein capacity. The K_d value follows the trend of the binding capacity and shows higher binding strength on bare membranes as the K_d values is smaller than in silica. Since greater amount of BSA was bound to bare and amine functionalized membranes than silica, thus K_d values were smaller for these two membranes than silica-coated membranes. Therefore, least strength of binding of BSA was observed on silica-coated membranes.

3.3.5 Water permeation tests on multiple protein fouled membranes

The adsorption of BSA and IgG to membrane surfaces leads to reduction in permeability of the membrane and represents a serious inefficiency of the membrane filtration operation. Factors such as protein adsorption, permeate flux and overall membrane fouling during adsorption of BSA and IgG using different membranes were studied by the water permeation test. All water permeation tests was performed by varying the pressure from 1 psi to 15 psi and the flow rate was measured with the pressure change for each of the membranes used after the adsorption isotherm test. Each trend line represents a single membrane with a different amount of protein adsorbed. Figures 3.7 and 3.8 show the results of the water permeation test performed with BSA and IgG adsorbed on bare

membrane respectively. Slopes for each trend line represent permeability of the membrane.

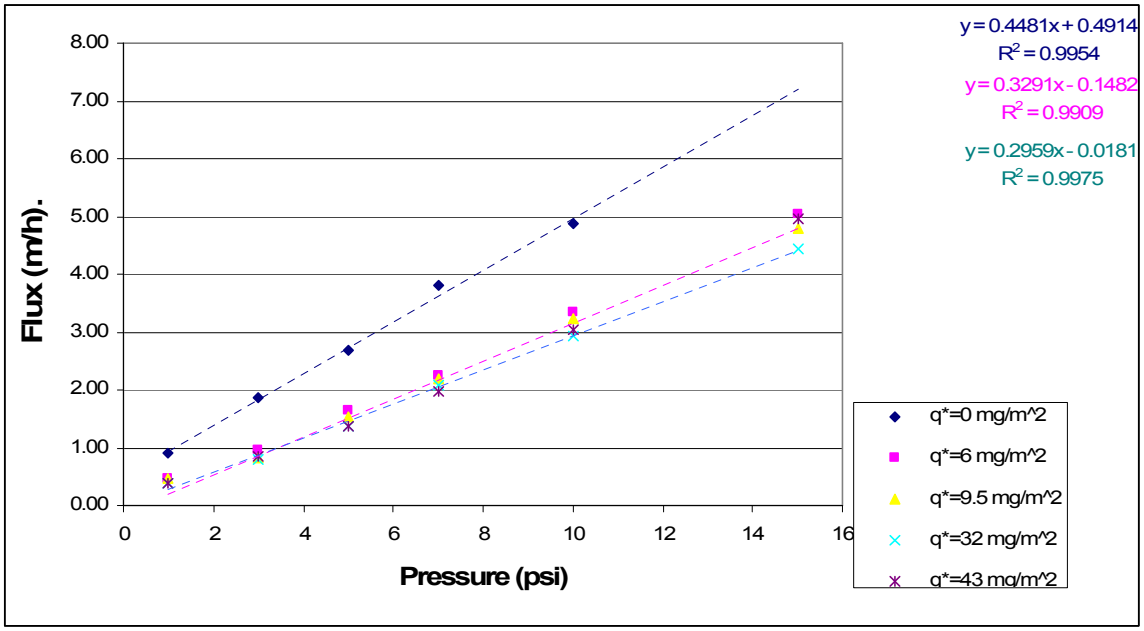

Figure 3.7 Flux vs. pressure for bare membranes fouled with BSA.

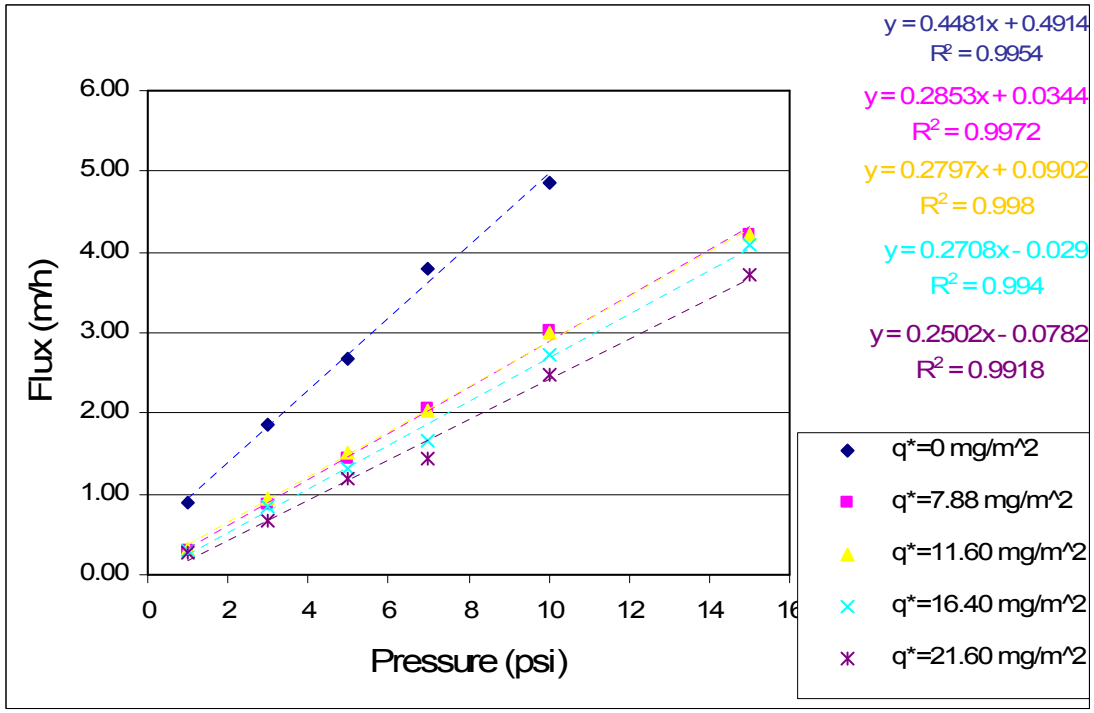

Figure 3.8 Flux vs. pressure for bare membranes fouled with IgG.

The results of water permeation tests on bare membranes with both BSA and IgG adsorption showed a decrease in the slope (permeability) when compared to the non-fouled membrane (Figures 3.7 and 3.8). In case of BSA fouled membrane, there is about 30% decrease in permeability for all the bare membranes. The permeability decrease did not significantly increase with the increase in the concentration of protein adsorbed on the membranes. That could be explained by a multilayer adsorption of BSA on the bare membrane that was easily removed during the initial washing of the membranes. In case of IgG fouled membrane, there was about 38%-46% decrease in the permeability of the bare membrane. In this case, the decrease in permeability was affected by the increase of adsorbed protein concentration (Figure 3.8).

Figures 3.9 and 3.10 show the results of the water permeation tests performed on BSA and IgG adsorbed to silica-coated membrane, respectively. As before, the slope of each trend line represents the permeability of the membrane.

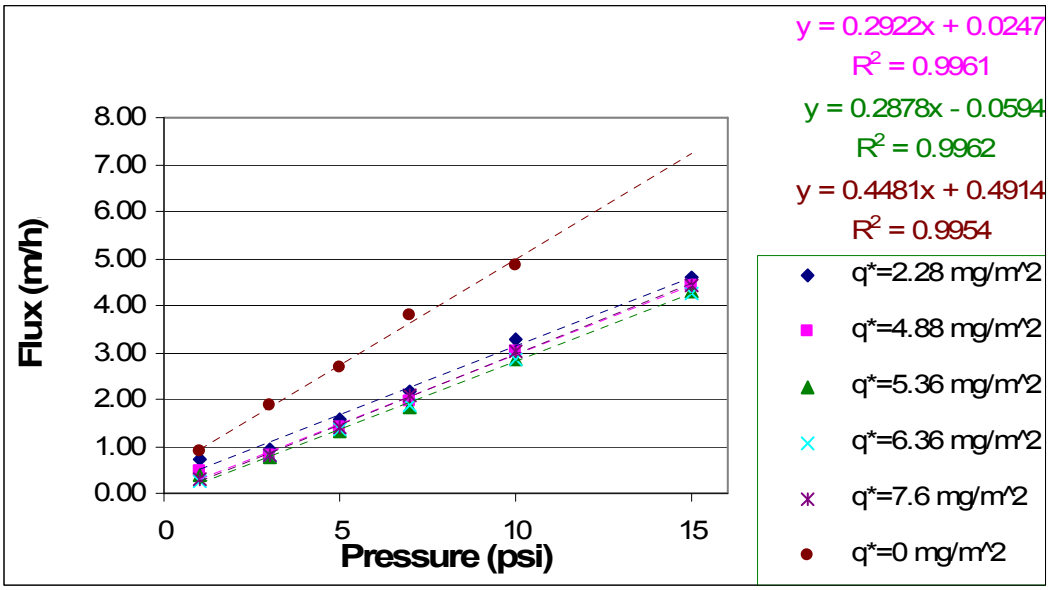

Figure 3.9 Flux vs. pressure for silica-coated membranes fouled with BSA.

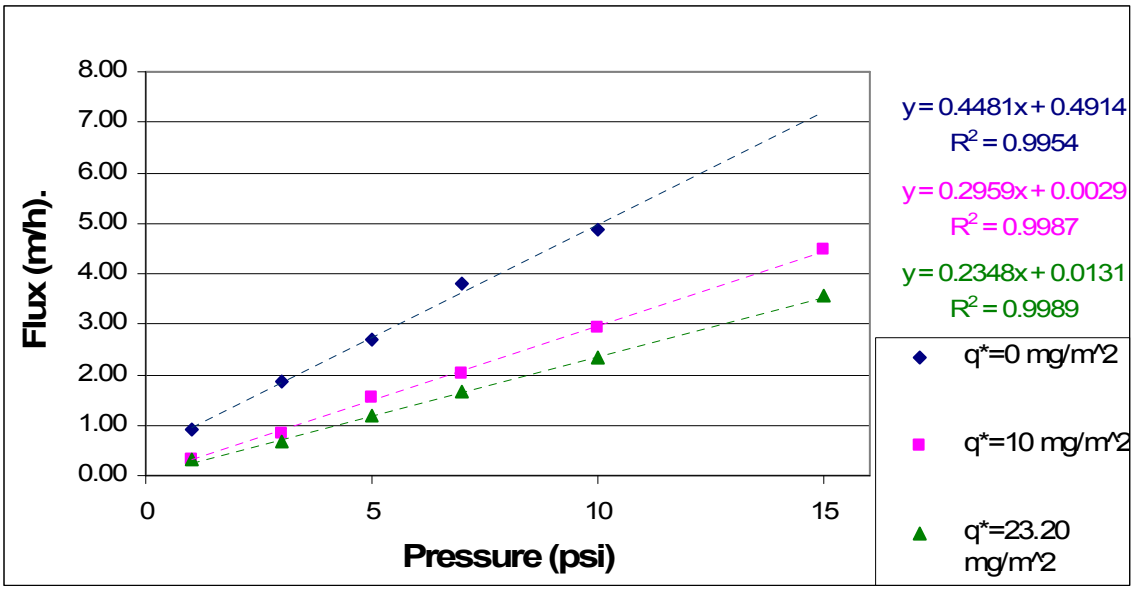

Figure 3.10 Flux vs. pressure for silica-coated membranes fouled with IgG.

The results of water permeation tests on silica-coated membranes with both BSA and IgG adsorption showed a decrease in the permeability when the membranes were fouled or had adsorbed protein (Figure 3.9 and 3.10). In the case of BSA fouled membrane, there was about 35% decrease in permeability of the silica-coated membranes. The permeability of the silica-coated membranes did not significantly decrease with an increase in the concentration of adsorbed protein. This behavior was similar to that of the bare membrane. The presumed multilayer BSA accumulation on the silica-coated membrane was easily removed during the initial washing of the membrane. With the IgG fouled membrane, there was 35%-48% decrease in the permeability of the silica-coated membrane (Figure 3.10). The permeability decreased significantly with an increase in the concentration of adsorbed protein.

Figures 3.11 and 3.12 show the results of the water permeation test performed with BSA and IgG adsorbed on amine-functionalized membrane, respectively.

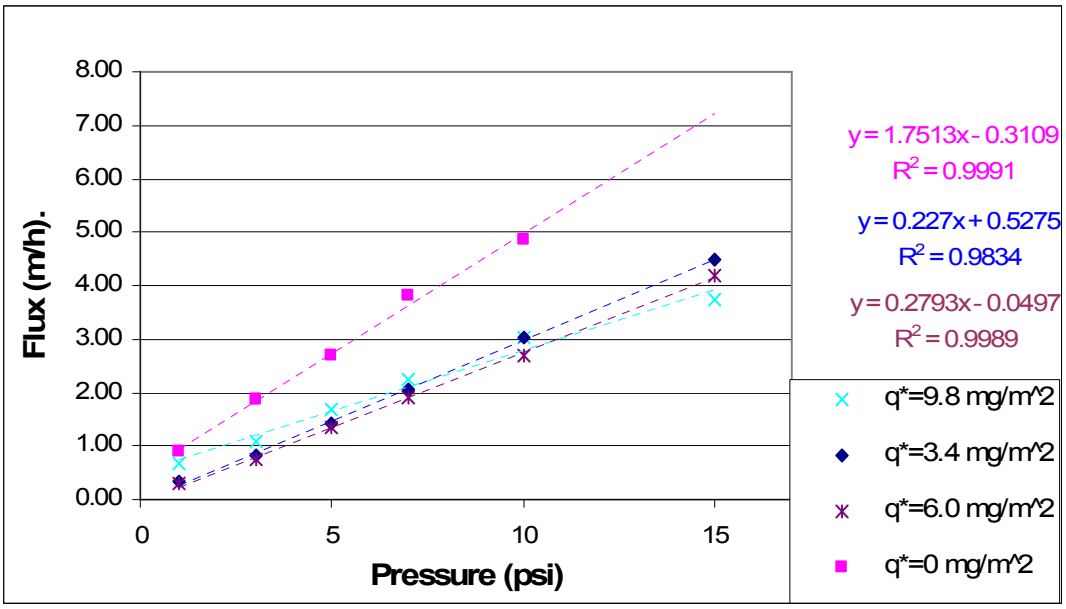

Figure 3.11 Flux vs. pressure for amine-functionalized membranes fouled with BSA.

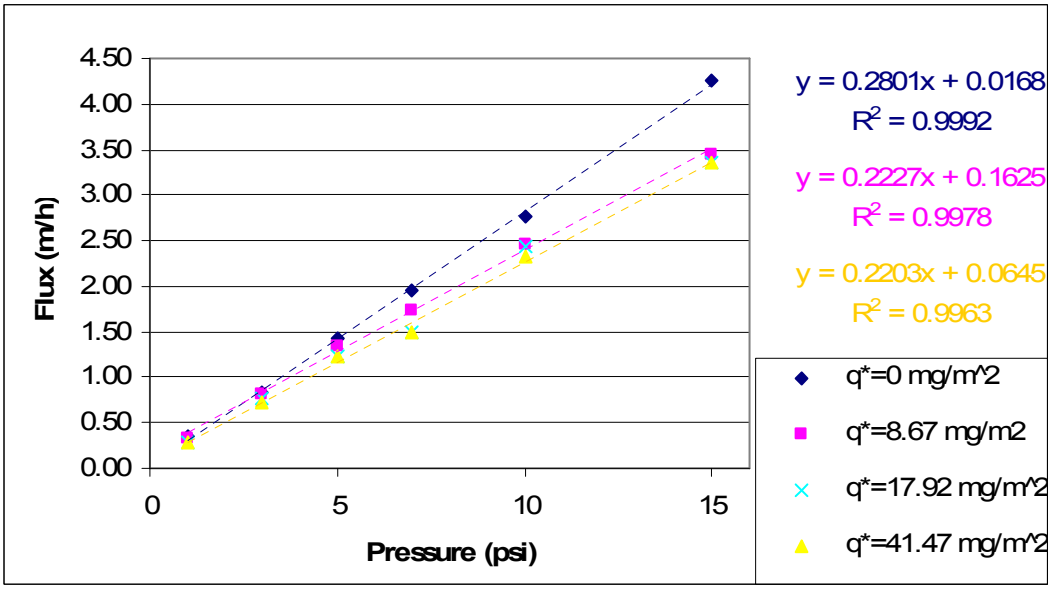

Figure 3.12 Flux vs. pressure for amine-functionalized membranes fouled with IgG.

The results of water permeation tests on amine-functionalized membranes with adsorbed BSA and IgG showed a decrease in the slope (permeability) compared to the non-fouled membrane (Figures 3.11 and 3.12). In the case of BSA fouled membrane, there was about 38-50% decrease in permeability. The permeability of amine-functionalized membranes significantly decreased with the increase in the concentration of protein adsorbed on to

the membranes. This trend could be explained by the specific adsorption of BSA on amine-functionalized membrane. In the case of IgG fouled membrane, there was 20% decrease in the permeability of the amine- functionalized membranes. The permeability did not decrease significantly with the concentration of adsorbed IgG probably because of the multi-layer deposition of IgG on amine-functionalized membranes.

3.3.6 Discussion on water permeation study

In all the cases, protein fouled membrane had a lower permeability than that of the non-fouled membranes. The pore size of bare membranes was 10-20% bigger than that of the functionalized membranes. Therefore, aggregated proteins could be removed from the pores during initial 2 minutes of washing in the permeation test. Protein concentration did not affect permeability for those membranes where there was no specific adsorption but, multi-layer proteins accumulation on the membrane surface. From all the permeation tests, it can be concluded that the permeate flux/ permeability (slope for each membrane) was a function of protein concentration and transmembrane pressure, a classic membrane filtration behavior. The previous studies of fouling, coupled with static adsorption studies, indicated that adsorption-related pore plugging plays a significant role in alumina microfiltration (*81*).

3.3.7 IgG binding to the protein A mimetic ligand membrane

Adsorption experiments of pure IgG, BSA and a 50:50 molar mixture of IgG and BSA were performed with different membranes to determine the selectivity of IgG binding. Figure 3.13 compares IgG and BSA adsorption on different membranes. The x-axis the initial adsorbed concentration, C_o of IgG on different membranes.

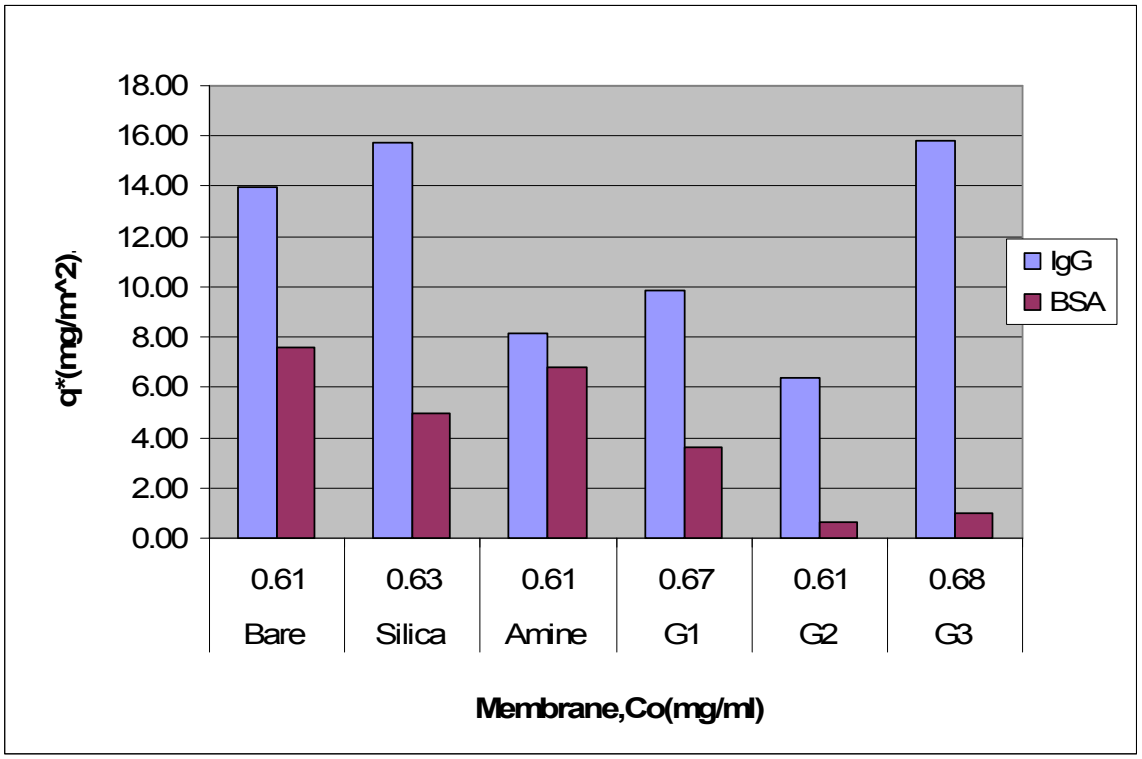

Figure 3.13 Comparison of IgG and BSA adsorption to different mimetic membranes.

The comparison of q* values for all the membranes showed that G3 mimetic membrane was the best for selective binding of IgG. G3 membranes had the highest amount of adsorbed IgG (15.8 mg/m^2) and very low amount of adsorbed BSA (1 mg/m^2) (Figure 3.13). G2 membrane also exhibited selectivity for IgG, as there was insignificant amount of adsorbed BSA bounded (0.67 mg/m^2), but the IgG bound to G2 membrane was less than half of G3 membrane. G1 in comparison with G2 and G3 membranes did not demonstrated good selectivity for IgG binding. Since the amount of protein A mimetic ligand on G1 was half the size of that on G2, there might still be open surface between the ligands on the membrane for both BSA and IgG to bind non-specifically. Therefore, there was still comparatively higher amount of BSA bound (3.59 mg/m^2) to G1 than G2 and G3 membranes. The greater amount of adsorbed IgG on G1 than G2 membrane probably resulted from the combined specific and non-specific binding.

From the adsorption data on the different membranes, selectivity for IgG was calculated as the ratio of IgG to BSA adsorption. Figure 3.14 shows the selectivity of IgG for differently modified membranes.

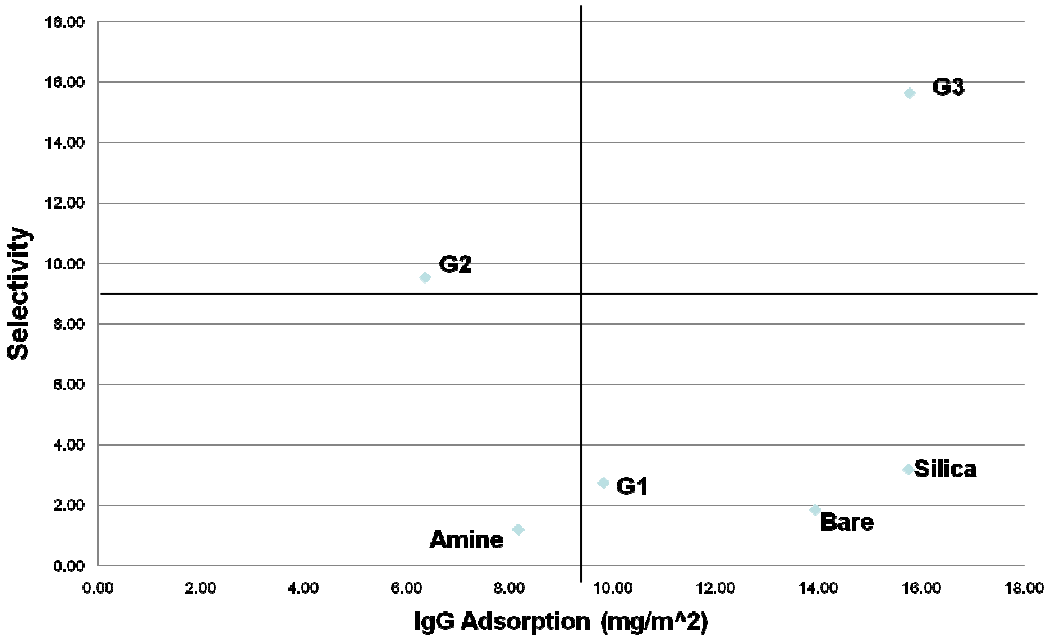

Figure 3.14 Membrane selectivity for binding of IgG.

G3 membrane had the highest selectivity and adsorption capacity for IgG compared with the rest of the membranes shown in Figure 3.14. G2 membrane had the second highest selectivity but IgG adsorption was not as high. The drawback of G1, bare, and silica-coated membranes was a significant non-specific BSA adsorption, therefore, a very low selectivity for IgG.

After the adsorption of IgG on protein A mimetic ligand membrane (G1, G2, and G3), protein desorption and recovery from G1-, G2- and G3-mimetic membranes was also investigated. IgG desorption from G1, G2 and G3 membranes was compared silica-coated membranes to determine if all of the adsorbed protein came off during the desorption process. Figure 3.15 shows desorption results for IgG and BSA from all G-mimetic membranes.

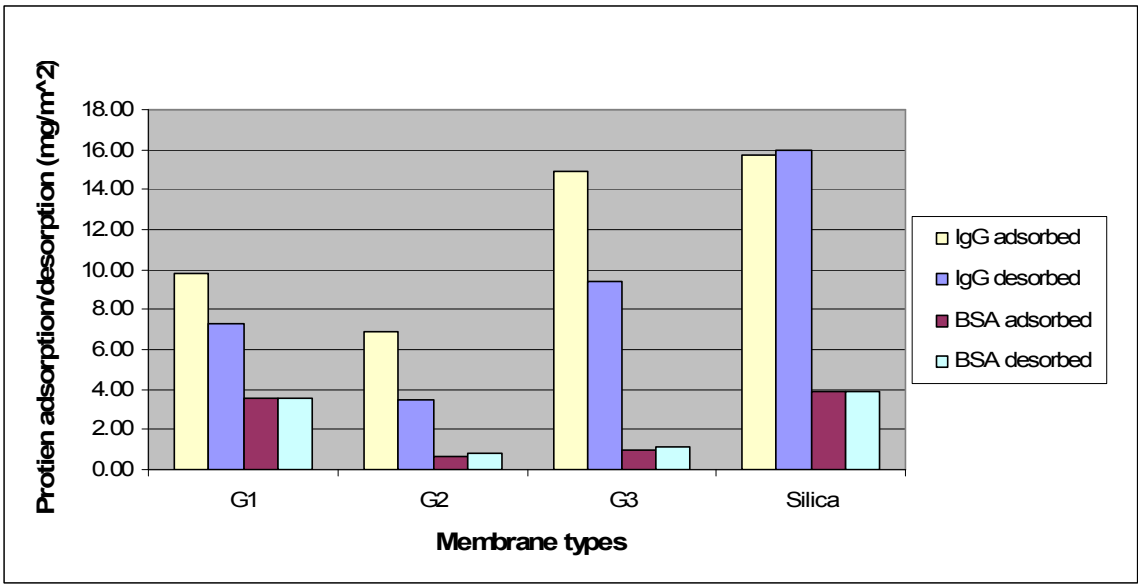

Figure 3.15 IgG and BSA adsorption and desorption in different membranes.

For G1, G2 and G3 membranes, IgG desorption was 75%, 50% and 63% respectively. BSA desorption was 100% for all the membranes indicating that BSA did not specifically interact with the protein A mimetic ligands (Figure 3.15). On the other hand, both proteins (IgG and BSA) came off from silica-coated membranes (Figure 3.15) during the desorption sequence. This information is an additional indirect confirmation that IgG binds selectively to the protein A mimetic ligands because it did not come off during the desorption process whereas silica-coated membranes resulted in 100% recovery of IgG.

Figure 3.16 summarizes the total amount of protein (IgG and BSA) adsorbed and desorbed for a 50:50 molar mixture. The protein desorption from the protein A mimetic ligand membranes was compared to the silica-coated membranes.

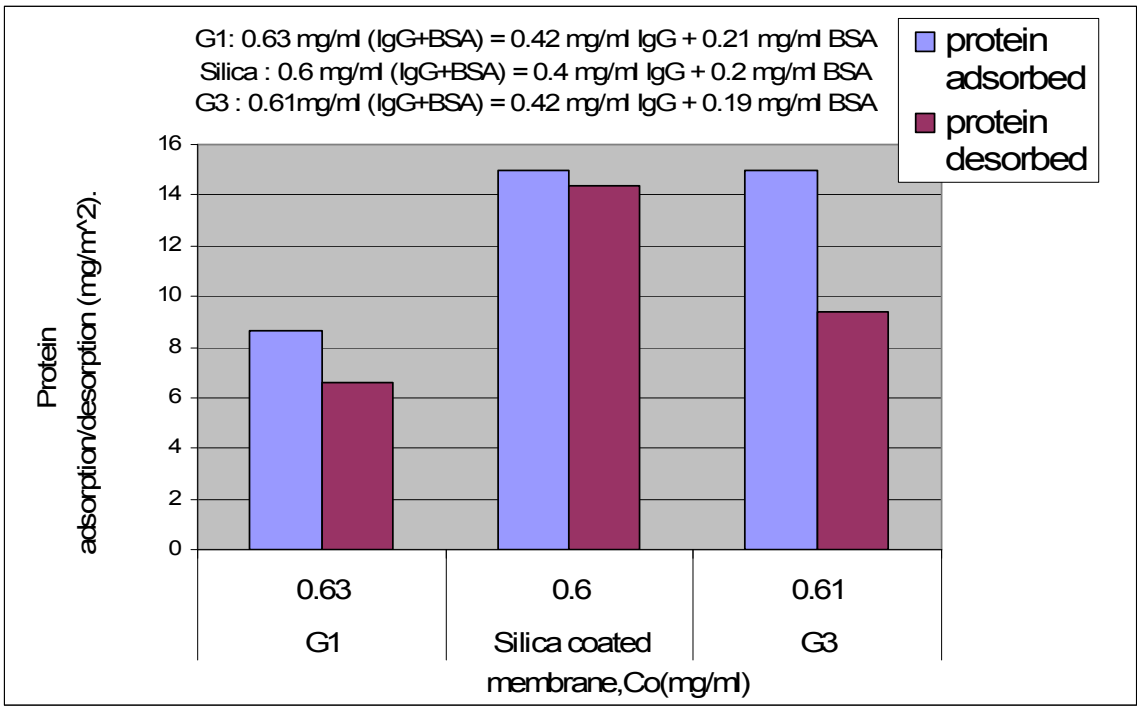

Figure 3.16 Adsorption and desorption of the 50:50 molar mixture of IgG and BSA.

For the 50:50 molar mixture of protein solution 76% of the total protein was desorbed from G1 membrane and 44% was desorbed from G3 membrane. Similar to experiments with pure proteins, almost 100% of bound protein was desorbed from silica-coated membrane. This difference reflects the inability to completely desorb specifically bound IgG from G1 or G3 membranes. Based on the pure IgG and BSA adsorption data, out of the 44% desorbed protein from the G3 membrane, only 2% (0.3 mg/m^2) was BSA and the rest was IgG (6.62 mg/m^2).

The desorption of IgG and BSA was analyzed by SDS-PAGE. The set of gels (Figure 3.17 and 3.18) show the elution profile for 50:50 molar mixture of IgG and BSA and a pure IgG from G3 membrane.

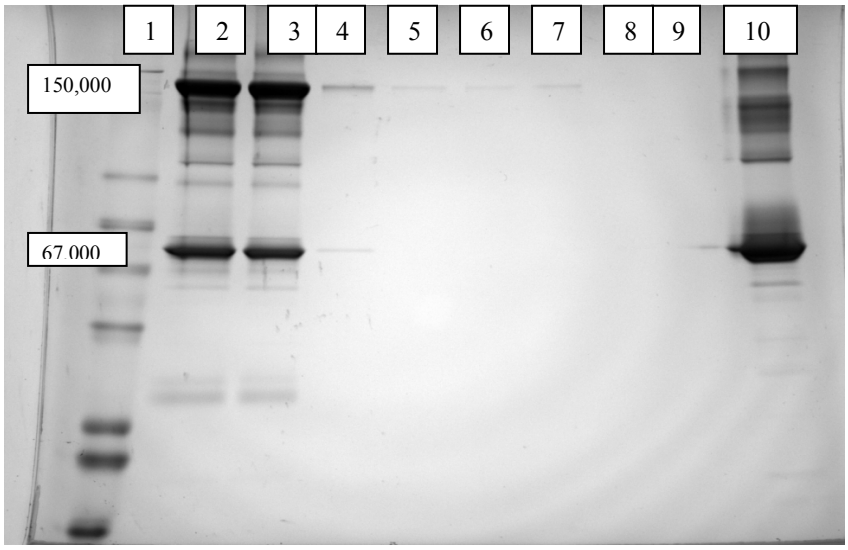

Figure 3.17 SDS-PAGE desorption profile of BSA and IgG mixture from G3 membrane. (Lane 1: MW Mark; Lane 2: Protein mixture before adsorption; Lane 3: Protein mixture after adsorption; Lane 4: PBS wash 1; Lane 5: PBS wash 2; Lane 6: NaCl wash; Lane 7: Citrate wash 1; Lane 8: Citrate wash 2; Lane 9: Citrate wash 3; Lane 10: BSA before adsorption)

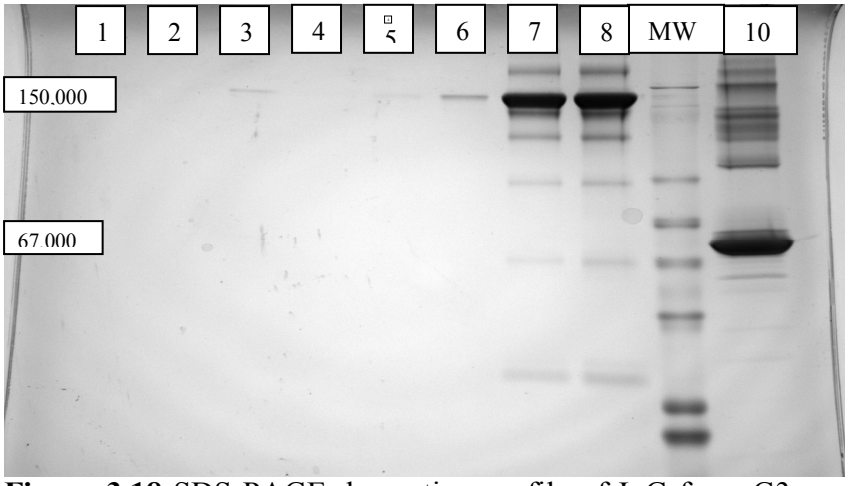

Figure 3.18 SDS-PAGE desorption profile of IgG from G3 membrane. (Lane 10: BSA after adsorption; Lane 9: MW Mark; Lane 8: IgG before adsorption; Lane 7: IgG after adsorption; Lane 6: PBS wash 1; Lane 5: PBS wash 2; Lane 4: NaCl wash; Lane 3: Citrate wash 1; Lane 2: Citrate wash 2; Lane 1: Citrate wash 3)

From Figure 3.17, Lanes 4 through 9 shows the elution of only IgG bands; No BSA was detected in these lanes. The presence of IgG bands in lanes 4-9, indicates that IgG is bound to the mimetic ligands, and some of it comes off during the desorption process. Any adsorbed BSA is removed in the first PBS wash (BSA band) and, thus, no BSA is being detected in the latter washes (no BSA band seen). BSA before and after adsorption on G3 membrane is shown in Figures 3.17 and 3.18, lane 10. There is no major difference in the two as BSA adsorption was not significant on G3 membranes. On Figure 3.18, lanes 3 through 6 (first few washes) IgG desorption is seen. Since the IgG desorption was very low in the last 2 washes, lane 1 and 2 do not show IgG desorption bands clearly.

3.3.8 Discussion on protein A mimetic ligand membrane interaction with IgG

All the results demonstrated higher binding capacity of G3 membranes to protein A mimetic ligands than G1 or G2 membranes. The primary binding site for protein A is on the Fc region of IgG (*66*). Previous research showed that an induced fit occurred between protein A and the Fc binding region on IgG which resulted in a very strong IgG - Protein A interaction (*83*). In case of G3 membranes, the denser population of the protein A mimetic ligands apparently enhances the interaction between IgG and the membrane. The affinity interactions between the protein A mimetic ligand and IgG are primarily hydrophobic in nature. The association between protein A mimetic ligands and IgG is probably stabilized by van der Waals interactions and hydrogen bonding. That could be the reason why using sodium chloride solution in one of the desorption steps did not help in the elution process.

3.4 Conclusion

Least fouling occurs with polyethylene glycol (PEG) membranes when BSA protein was used. Amine-functionalized membranes showed specific interaction (electrostatic attraction) with BSA and Langmuirian adsorption behavior. Bare and silica coated membrane (electrostatic repulsion) did not have specific interaction with BSA as there was multi-layer formation. IgG had higher adsorption thus fouling than BSA on all the membranes. IgG adsorption on amine functionalized membranes did not follow Langmuir behavior and there was multi-layer deposition of IgG. Bare and silica coated membranes had lower IgG adsorption than amine functionalized membrane. G3 membrane synthesized to selectively bind IgG is a noble option to separate IgG from a protein mixture. BSA bound to the protein A mimetic ligand membrane were not significant.

CHAPTER IV

CONCLUSION AND RECOMMENDATION

Buffer, pH and rice extract impurity, phytic acid affects lysozyme adsorption on SP Sepharose. Binding capacity and strength are significantly affected by phytic acid in all buffers. Removing phytic acid from rice extract may be a good option for increasing lysozyme binding capacity to SP Sepharose.

Fouling is decreased significantly by changing the surface properties of the alumina membranes. Least fouling occurs with polyethylene glycol (PEG) membranes when BSA protein is used. IgG has higher adsorption thus fouling than BSA on all the membranes. G3 membranes are a good option to selectively bind IgG from a protein mixture. BSA bound to the protein A mimetic ligand membrane is not significant.

REFERENCES

(1) Goldstein, D.A.; Thomas, J.A. Biopharmaceuticals derived from genetically modified plants. *Q.J. Med*. **2004**, *97*, 705-716.

(2) Wilken, L.; Nikolov, Z. L.; Factors influencing recombinant human lysozyme extraction and cation exchange adsorption. *Biotechnol. Prog.* **2006**, *22*, 745-52.

(3) Menkhaus, T. J.; Bai, Y.; Zhang, C.; Nikolov, Z. L.; Glatz, C. E. Considerations for the recovery of recombinant proteins from plants. *Biotechnol. Prog.* **2004**, *20*, 1001-1014.

(4) Yandi, D.; Chang, Q.; Charles, E. G. Recovery of enzyme byproducts from potential plant hosts for recombinant protein production. *Enzyme Microb. Technol.* **2003,** *33*, 596-605.

(5) Nikolov, Z. L.; Woodard, S. L.; Downstream processing of recombinant proteins from transgenic feedstock. *Curr. Opin. Biotechnol*. **2004**, *15*, 479-486.

(6) Ma, J. K-C.; Drake, P. M.; Christou, P. The production of recombinant pharmaceutical proteins in plants. *Nat. Rev. Genet*. **2003**, *4*, 794-805.

(7) Humphrey, B.; Huang, N.; Klasing, K. C. Rice expressing lactoferrin and lysozyme has antibiotic-like properties when fed to chicks. *J. Nutr.* **2002,** *132*, 1214-1218.

(8) Nandi, S.; Suzuki, Y. A.; Huang, J.; Yalda, D.; Pham, P.; Wu, L.; Bartley, G.; Huang, N.; Lonnerdal, B. Expression of human lactoferrin in transgenic rice grains for the application of infant formula. *Plant Sci*. **2002**, *163*, 713-722.

(9) Proctor, V. A.; Cunningham, F. E.; Fung, D. Y. C. The chemistry of lysozyme and its use as a food preservative and a pharmaceutical. *Food Sci. Nutr.* **1988**, *26*, 359-395.

(10) Ellison, R. T.; Giehl, T. J. Killing of gram-negative bacteria by lactoferrin and lysozyme. J. Clin. Investig. 1991, 88, 1080-1091.

(11) Abe, H.; Saito, H.; Miyakawa, H.; Tamura, Y.; Shimamura, S.; Nagao, E.; Tomita, M. Heat stability of bovine lactoferrin at acidic pH. *J. Dairy Sci*. **1991**, *74*, 65-71.

(12) Eschenburg, G.; Heine, W.; Peters, E.; Fecal sigS and lysozyme excretion in breast feeding and formula feeding. *Kinderaerzti.* **1990**, *58*, 255-260.

(13) Kuwata, H.; Yamauchi, K.; Teraguchi, S.; Ushlda, Y.; Shlmokawa, Y.; Tolda, T.; Hayasawa, H.; Functional frangments of ingested lactoferrin are resistant to

proteolytic degradation in the gastrointestinal tract of adult rats. *J. Nutr*. **2001**, *131*, 2121-2127.

(14) Troost, F.; Steinjs, J.; Saris, W.; Brummer, R. Gastric digestion of bovine lactoferrin in vivo in adults. *J. Nutr*. **2001**, *131*, 2101-2104.

(15) Juliano, B. O. *Rice*: *Chemistry and Technology*; American Association of Cereal Chemists, Inc.: St. Paul, MN, 1985.

(16) Cheryan, M. Phytic acid interactions in food systems. *CRC Crit. Rev. Food Sci. Nutr.* **1980**, *13*, 297-335.

(17) Liang, J.; Han, B.; Han, L.; Nout, R.; Hamer, R. Iron, zinc and phytic acid content of selected rice varieties from China. *J. Sci. Food Agric.* **2006**, *87*, 504-510.

(18) Hurrell, R. F. Influence of vegetable protein sources on trace element and mineral bioavalability. *J Nutr*. **2003,** *133*, 2973S-2977S.

(19) Hidvegi, M.; Lasztity, R. Phytic acid content of cereals and legumes and interaction with proteins. *Periodica Polyt. Ser. Chem. Engr.*. **2002**, *46*, 59-64.

(20) Lasztity, R.; Lasztity, L. Investigation of the formation of phytate-metal complexes. *Periodica Polyt.* **1988**, *32*, 299-304.

(21) Reddy, N. R.; Sathe, S. K.; Salunkhe, D. K. Phytates in legumes and cereals. *Adv. Food Res.* **1982**, *28*, 1-92.

(22) Tsuchiya, Y.; Morioka, K.; Shirai, J.; Yoshida, K. Establishment of a mass production system for human lysozyme as curative medicine to AIDS. *Int. Conf. AIDS*. **2004**, *15*, 11-16.

(23) Smith, G.; Stoker, C. Inhibition of crystalline lysozyme. *Biochem. Biophys. Acta* **1949**, *21*, 302-383.

(24) Hunter, J. J.; Volschenk, C. G.; Marais, J.; Fouche, G. W. Composition of Sauvignon blanc grapes as affected by pre-v,raison canopy manipulation and ripeness level. *S. Afr. J. Enol. Vitic.* **2004**, *25*, 13-18.

(25) Odabasi, M.; Say, R.; Denizli, A. Molecular imprinted particles for lysozyme purification. *Mater. Sci. Eng*. **2007**, *27*, 90-99.

(26) Ghosh, R.; Silva, S.S.; Cui, Z. F. Lysozyme separation by hollow fibre ultrafiltration. *Biochem. Eng. J*. **2000**, *6*, 19-24.

(27) Huang, J.; Wu, L.; Yalda, D.; Adkins, Y.; Kelleher, S.L.; Crane, M.; Lonnerdal, B.; Rodriguez, R. L.; Huang, N. Expression of functional recombinant human lysozyme in transgenic rice cell culture. *Transgenic Res*. **2002**, *11*, 229-239.

(28) Hashim, M.A.; Chu, K-H.; Tsan, P-S.; Effects of ionic strength and pH on the adsorption equilibria of lysozyme on ion exchangers. *J. Chem. Tech. Biotechnol.* **1994**, *62*, 253-260.

(29) Harrison, R.; Todd, P.; Rudge, S.; Petrides, D. *Bioseparations Science and Engineering*; Oxford University Press: New York, 2003.

(30) Huang, J.X.; Schudel, J.; Guiochon, G. Adsorption behavior of albumin and conalbumin on TSK-DEAE 5PW anion exchanger. *J. Chromatogr*. **1990**, *504*, 121-128.

(31) James, E. A.; Do, D. D. Equilibria of biomolecules on ion-exchange adsorbents. *J. Chromatogr*. **1991**, *542*, 19-28.

(32) Srikanth, G. Membrane separation processes- technology and business opportunities. http://www.biologica.eng.uminho.pt/PSB/docs/TextoFicha3.pdf. **2008**. 10/9/2008.

(33) Matthias, F.; Martin, S. H.; Timothy, H.; Owen, T. Protein purification using magnetic adsorbent particles. *Appl. Microbiol. Biotechnol*. **2006**, *70*, 505-516.

(34) Van Reis, R.; Zydney, A. L. Membrane separations in biotechnology. *Curr. Opin. Biotechnol.* **2001,** *12*, 208-211.

(35) Burns, D.B.; Zydney, A. L. Effect of solution pH on protein transport through semipermeable ultrafiltration membranes. *Biotechnol. Bioeng.* **1999,** *64*, 27-37.

(36) Ebersold, M. F.; Zydney, A. L. The effect of membrane properties on the separation of protein charge variants using ultrafiltration. *J. Membr. Sci.* **2004,** *243*, 379-388.

(37) Ghosh, R. Q.; Wan, Y.; Cui, F. Separation of human. serum albumin and human immunoglobulins using nonlinear control techniques. *AIChE J.* **1998,** *44*, 61-67.

(38) Matto, M.; Rice, C. M.; Aroeti, B.; Glenn, J. S. Hepatitis C virus core protein associates with detergent-resistant membranes distinct from classical plasma membrane rafts. *J. Virol.* **2004**, *78*, 12047-12053.

(39) Teng, M. Y.; Lin, S. H.; Wu, C. Y.; Juang, R. S. Factors affecting selective rejection of proteins within a binary mixture during cross-flow ultrafiltration. *J. Membr. Sci.* **2003**, *281*, 103-110.

(40) Van Reis, R.; Gadam, S.; Frautschy, L. N.; Orlando, S.; Goodrich, E. M.; Saksena, S.; Kuriyel, R.; Simpson, C. M.; Pearl, S.; Zydney, A. L. High performance tangential flow filtration. *Biotechnol. Bioeng.* **1997**, *56*, 71-82.

(41) Ho, C. C.; Zydney, A. L. Theoretical analysis of the effect of membrane during microfiltration. *J. Colloid Interface Sci.* **2000,** *232*, 389-399.

(42) Palacio, L.; Ho, C. C.; Zydney, A. L. Application of a pore blockage - cake filtration model to protein fouling during microfiltration. *Biotechnol. Bioeng.* **2002,** *79*, 260-270.

(43) Palacio, L.; Ho, C. C.; Pradanos, P.; Hernandez, A.; Zydney, A. L. BSA-lysozyme and BSA-pepsin. *J. Membr. Sci.* **2003,** *222*, 41-51.

(44) Nakamura, K.; Matsumoto, K.; Spinett, R. F. Fouling of hydrophobic microfiltration membrane by algae and algal organic matter: mechanisms and prevention. *J. Membr. Sci.* **2006,** *285*, 126-136.

(45) Bowen, W. R.; Gan, Q. Properties of microfiltration membranes: flux loss during constant pressure permeation of bovine serum albumin. *Biotechnol. Bioeng*. **1991**, *38*, 688-696.

(46) Kelly, S.T.; Zydney, A. L. Protein fouling during microfiltration: comparative behavior of different model proteins. *Biotechnol. Bioeng*. **1997**, *55*, 91-100.

(47) Martin, A.; Martinez. R.; Calvo, J. J.; Pradanos, P.; Palacio, L.; Hernandez, A.; Protein surface coverage. *J. Membr. Sci.* **2002**. *207*. 199-327.

(48) Mochizuki, S.; Zydney, A. L.; Opong, W. S. Macromolecular sieving by protein deposits formed during ultrafiltration and microfiltration. *Proceedings of the International Congress on Membranes and Membrane Technol*. **1990**, *2*, 1137-1139.

(49) Robertson, B. C.; Zydney, A. L. Hindered protein diffusion in asymmetric ultrafiltration membranes with highly constricted pores. *J. Membr. Sci.* **1990**, *49*, 287-303.

(50) Pitt, A. M. The non-specific binding of polymeric microporous membranes. *J. Parenteral Sci. Technol*. **1987**, *41*, 110-113.

(51) Zeng, X.; Ruckenstein, E. Membrane chromatography: preparation and applications to protein separation. *Covance Biotechnol. Serv.* **1999**, *15*, 1003-1019.

(52) Finger, U. B.; Thömmes, J.; Kinzelt, D.; Kula, M. R. Application of thiophilic membranes for the purification of monoclonal antibodies from cell culture media. *J. Chromatogr. B.* **1995,** *664*, 69-74.

(53) Arica, M. Y.; Yalçin, E.; Bayramoglŭ, G. Affinity membrane chromatography: relationship of dye-ligand type to surface polarity and their effect on lysozyme separation and purification. *J. Chromatogr. B.* **2004**, *805*, 315-323.

(54) Mochizuki, S.; Zydney, A. L. Effect of protein adsorption on the transport characteristics of asymmetric ultrafiltration membranes. *Biotechnol. Prog.* **1992**, *8*, 553-561.

(55) Ghosh, R. Protein separation using membrane chromatography: opportunities and challenges. *J. Chromatogr. A.* **2002**, *952*, 13-27.

(56) Laemmli, U. K. Cleavage of structural proteins during the assembly of the head of bacteriophage T4. *Nat. Rev. Genet.* **1970**, *227*, 680-685.

(57) Thompson, W. R.; Pemberton, J. E. Raman spectroscopy of covalently bonded alkyl silane layers on thin silica immobilized on silver substrates. *Langmuir.* **1995,** *11*, 1720-1725.

(58) Beier, S.P.; Enevoldsen, A. D.; Kontogeorgis, G. M.; Hansen, E. B.; Jonsson, G. Adsorption of amylase enzyme on ultrafiltration membranes. *Langmuir.* **2007**, *23*, 9341-9351.

(59) Marshall. A. D.; Munro, P. A.; Tragardh, G.; The effect of protein fouling in microfiltration and ultrafiltration on permeate flux, protein retention and selectivity: a literature review. *Desalination*. **1993**, *91*, 65-108.

(60) Kelly, S. T.; Opong, W. S.; Zydney, A. L. The influence of protein aggregates on the fouling of microfiltration membranes during stirred cell filtration. *J. Membr. Sci.* **1993**, *80*, 175-187.

(61) Mulder, M. *Book Review: Basic Principles of Membrane Technology*; Institute of Biotechnology: Jülich, Germany, 1997.

(62) Zhou, J. X.; Tresses, T. Basic concepts in Q membrane chromatography for large-scale antibody production. *AIChE J.* **2006**, *10*, 1021-1030.

(63) Zydney, A.L.; Pujar, N. S. Protein transport through porous membranes: effect of colloidal interactions. *Colloids Surfaces. A: Physicochem. Eng. Aspects*. **1998**, *138*, 133-143.

(64) Chadd, H. E.; Chamow, S. M. Therapeutic antibody expression technology. *Curr. Opin. Biotechnol*. **2001**, *12*, 188-194.

(65) Walsh, G. Biopharmaceuticles: approvals and approval trends in 2004. *Bio Pharm Int.* **2005**, *18*, 58-65.

(66) Yahiro, U.; Kazumi, F.; Takashi, K.; Yoshiaki, K.; Ryutaro, Y.; Eiji, K.; Tomokuni, T.; Kazuaki, N.; Masahiro, W.; Masayuki, N.; Tadakazu, S. Monoclonal antibody, process for preparing same, reagent for detecting cancer antigen containing the monoclonal antibody and process for preparing same. U. S. Patent Application 4959320, 1990.

(67) Li, F.; Zhou, J.; Yang, X.; Tressel, T.; Lee, B. Current therapeutic antibody production and process optimization. *Bioprocess J*. **2005**, *4*, 23-30.

(68) Gagnon, P.; Hensel, F.; Richieri, R. *Advances in Separation and Purification: Purifying Monoclonal Antibodies*; An Advanstar Publication: Foster City, CA, USA, 2008.

(69) Belfort, G.; Davis, R. H.; Zydney, A. L. The behavior of suspensions and macromolecular solutions in crossflow microfiltration. *J. Membr. Sci*. **1994**, *96*, 1-58.

(70) Li, R.; Dowd, V.; Stewart, D. J.; Burton, S. J.; Lowe, C. R. Protein A mimetic ligands. *Nat. Biotechnol.* **1998**, *16*, 190-195.

(71) Bradford, M. M. A rapid and sensitive method for the quantification of microgram quantities of protein utilizing the principle of protein dye binding. *Anal. Biochem*. **1976**, *72*, 248-254.

(72) Barlow, D. J.; Thornton, J. M. The distribution of charged groups in proteins. *Biopolym*. *Sci.* **1986**, *25*, 33-1717.

(73) Lesins, V.; Ruckenstein, E. Patch controlled attaractive electrostatic interactions between similarly charged proteins and adsorbents. *Colloid Polym. Sci*. **1988**, *266*, 90-1187.

(74) Kamyshny, A.; Lagerge, S.; Partyka, S.; Relkin, P.; Magdassi, S. Adsorption of native and hydrophobized human IgG onto silica: isotherms, calorimetry, and biological activity. *Langmuir*. **2001**, *17*, 8242-8248.

(75) Magdassi, S.; Kamyshny, A. *In Surface Activity of Proteins: Chemical and Physiochemical Modifications*; Marcel Dekker: New York, 1996.

(76) Haynes, C. A.; Norde, W. Globular proteins at solid/liquid interfaces. *J. Colloids Surf. B*. **1994**, *2*, 517-521.

(77) Haynes, C. A.; Norde, W. Reversibility and the mechanism of protein probed by atomic force microscopy. *J. Colloid Interface Sci*. **2002**, *23*, 153-164.

(78) Su, T. J.; Lu, J. R.; Thomas, R. K.; Cui, Z. F.; Penfold, J. The adsorption of lysozyme at the silica-water interface: a neutron reflection study. *J. Colloid Interface Sci.* **1998**, *203*, 419-429.

(79) Ho, C. C.; Zydney, A. L. Overview of fouling phenomena and modeling approaches for membrane bioreactors. *Sep. Sci. Tech*. **2006**, *41*, 1231-1253.

(80) Martinez, F.; Martina, A.; Pradanos, P.; Calvo, J.; Palacio, L.; Hernandez, A. Protein adsorption and deposition on to microfiltration membranes: the role of solute-solid interactions. *J. Colloid Interface Sci.* **2000**, *221*, 254-261.

(81) Ryosuke, T.; Masayuki, N. Characterization of the membrane charge of Al_2O_3 membranes. *J. Membrane Sci.* **2001**, *25*, 369-377.

(82) Kusakabe, K.; Ichiki, K.; Hayashi, J.; Maeda, H.; Morooka, S. Preparation and characterization of silica-polyimide composite membranes coated on porous tubes for CO_2 separation. *J. Membrane Sci.* **1996**, *115*, 65-75.

(83) Schröder, A. K.; Nardella, F. A.; Mannik, M.; Svensson, M. L.; Christensen, P. Interaction between streptococcal IgG Fc receptors and human and rabbit IgG domains. *Immunology*. **1986**, *57*, 305–309.

(84) Kenausis, G.L.; Voros, J.; Elbert, D. L.; Huang, N. P.; Hofer, R.; Ruiz-Taylor, L.; Textor, M.; Hubbell, J. A.; Spencer, N. D. Poly(L-lysine)-g-poly(ethylene glycol) layers on metal oxide surfaces: attachment mechanism and effects of polymer architecture on resistance to protein adsorption. *J. Phys. Chem. B*. **2000,** *104*, 3298-3309.

(85) Popat, K. C.; Mor, G.; Grimes, C.; Desai, T. A. The influence of PEG architecture on protein adsorption and conformation. *J. Membr. Sci.* **2004,** *243*, 97-106.

(86) Cecchet, F.; Meersman, B. D.; Demoustier-Champagne, S.; Nysten, B.; Jonas, A. M. One step growth of protein antifouling surfaces: monolayers of poly(ethylene oxide) (PEO) derivatives on oxidized and hydrogen-passivated silicon surfaces. *Langmuir.* **2006,** *22*, 1173-1181.

(87) Huang, N. P.; Michel, R.; Voros, J.; Textor, M.; Hofer, R.; Rossi, A.; Elbert, D. L.; Hubbell, J. A.; Spencer, N. D. Poly(L-lysine)-g-poly(ethylene glycol) layers on metal oxide surfaces: surface-analytical characterization and resistance to serum and fibrinogen adsorption. *Langmuir.* **2001**, *17*, 489-498.

(88) Ma, Q.; DeMarte, L.; Wang, Y.; Stanners, C. P.; Junghans, R. P. Carcinoembryonic antigen-immunoglobulin Fc fusion protein (CEA-Fc) for identification and activation of anti-CEA immunoglobulin-T-cell receptor-modified T cells, representative of a new class of Ig fusion proteins. *Cancer Gene Ther.* **2004**, *11*, 297-306.

APPENDIX A

TABLE A.1 ACETATE BUFFER AT pH 4.5, 9.7 mS LZ ADSORPTION DATA

Co (mg/ml)	C* (mg/ml)	q*(mg/ml)
0	0	0
0.28	0.0002	9.8
0.38	0.0003	12.5
0.54	0.0010	21.6
0.69	0.0012	24.0
1.45	0.0035	32.0
0.72	0.0047	35.0
0.89	0.012	43.5
2.27	0.0300	51.4
1.90	0.0480	55.0
2.96	0.087	61.0
2.45	0.116	63.0
3.20	0.438	81.1
3.61	0.4	78.0
4.38	1.035	90.4
5.11	1.67	91.0
5.42	1.44	91.0
6.15	3.02	96.0
6.22	2.20	93.3
6.72	2.75	96.7
6.80	3.45	95.8
7.64	3	99.0
6.80	3.45	95.8
7.64	3	99.0
6.80	3.45	95.8
7.64	3	99.0
8.96	5.52	100.0

TABLE A.2 ACETATE BUFFER AT pH 4.5, 12.6 mS LZ ADSORPTION DATA

Co (mg/ml)	C* (mg/ml)	q*(mg/ml)
0.36	0.0054	27.28
0.651	0.0057	34.71
1.1976	0.0197	46.37
2.01	0.43	69.30
2.8776	1.29	80.18
3.6124	1.878	82.59
4.62	2.46	87.10

TABLE A.3 ACETATE BUFFER AT pH 4.5, 9.7 mS LZ AND PHYTIC ACID ADSORPTION DATA

Co(mg/ml)	C* (mg/ml)	q*(mg/ml)
	0	0
0.350	0.0011	6.9
0.421	0.0035	7.4
0.559	0.0038	10.8
0.612	0.0041	11.6
0.987	0.0070	21.3
1.062	0.0049	19.99
1.286	0.0055	18.8
1.984	0.023	39.2
2.027	0.0065	26.4
3.001	0.064	52.5
3.152	0.020	41.1
3.564	0.036	43.1
3.614	0.083	51.9

TABLE A.4 PHOSPHATE BUFFER AT pH 6, 12.6 mS LZ ADSORPTION DATA

Co(mg/ml)	C* (mg/ml)	q*(mg/ml)
0.18	0.0066	3.0
0.34	0.0169	6.4
0.43	0.0298	11.5
0.54	0.036	12.5
0.74	0.05	13.9
1.01	0.059	16.0
0.95	0.071	15.2
1.56	0.15	28.2
2.05	0.24	40.0
2.35	0.396	46.0
3.04	0.581	52.0
3.44	1.02	59.0
4.17	1.128	61.0
4.5	1.46	65.0
4.51	1.49	64.0
5.81	1.75	69.6
5.36	2.33	70.0
6.59	2.42	72.0
6.42	2.86	72.0
7.91	3.6	72.4
7.64	3.79	78.5

TABLE A.5 PHOSPHATE BUFFER AT pH 6, 12.6 mS LZ AND PHYTIC ACID ADSORPTION DATA

Co (mg/ml)	C* (mg/ml)	q*(mg/ml)
0.18	0.02	2.8
0.37	0.01	6.2
0.398	0.020	5.92
0.406	0.023	5.87
0.46	0.03	8.40
0.58	0.03	9.2
0.840	0.049	11.3
0.991	0.078	14.1
0.83	0.08	12.9
1.00	0.11	16.7
1.09	0.08	17.0
1.85	0.32	26.0
1.89	0.26	30.0
2.27	0.32	32.1
2.89	0.63	40.0
2.84	0.73	42.1
2.95	0.98	44.3
3.13	1.06	42.0
4.03	2.20	45.0
4.13	1.53	49.9
4.05	1.33	52.0
4.68	1.67	54.0
4.99	1.81	54.1
5.19	1.72	55.6
5.51	2.11	55.7
6.26	2.11	58.0
6.27	2.17	68.0
7.61	2.68	73.0

TABLE A.6 TRIS BUFFER AT pH 6, 12.6 mS LZ ADSORPTION DATA

Co(mg/ml)	C*(mg/ml)	q*(mg/ml)
0	0	0
0.2508	0	4.2653061
0.5262	0.002	12.190698
0.8622	0.0011	14.846552
1.2558	0.013	26.555556
1.698	0.0343	32
2.1	0.0695	35.25
2.352	0.105	40.125
2.667	0.1353	45.86413
3.267	0.28	59.705285
3.4089	0.378	65.040773
4.356	0.9493	79.225581
5.55	1.6885	87.364253

TABLE A.7 TRIS BUFFER AT pH 6, 12.6 mS LZ AND PHYTIC ACID ADSORPTION DATA

Co(mg/ml)	C*(mg/ml)	q*(mg/ml)
0.4464	0.01	6.888013
0.602	0.026	11.35
0.3806	0.042	15.82243
1.017	0.08	19.3
1.2	0.09	23.85
0.7513	0.1378	28.40278
1.4373	0.16	30.2
1.14	0.35	35.9
2.5488	0.38	40
1.28	0.47	42.5
1.99	1.02	51.4
3.87	1.09	50
2.5014	1.3706	50.93694
4.6019	1.46	55
2.8765	1.5895	60
5.763	1.98	67.05496
3.63	2.2374	66.31429
3.939	2.42	69.04545
4.301	2.442	69.36567
6.12	2.67	51.99548

APPENDIX B

TABLE B.1 BARE MEMBRANE ADSORPTION DATA WITH BSA

Abs	Co(mg/ml)	Abs	C*(mg/ml)	Q*(mg/m^2)
0.056	0.28	0.049	0.203	5.37
0.086	0.32	0.0436	0.231	5.93
0.150	0.57	0.141	0.4625	7.33
0.199	0.78	0.172	0.655	8.00
0.1833	0.96	0.169	0.833	8.40
0.298	1.55	0.289	1.4105	9.57
0.431	2.24	0.426	2.044	12.83
0.412	3.74	0.629	3.255	32.20
0.789	4.15	0.78	3.605	36.17
0.527	4.75	0.784	4.1125	42.63
0.6251	5.676	1.26	4.875	53.40

TABLE B.2 SILICA COATED MEMBRANE ADSORPTION DATA WITH BSA

Abs	Co(mg/ml)	Abs	C*(mg/ml)	q*(mg/m^2)
0.03	0.29	0.03	0.26	2.28
0.07	0.58	0.05	0.51	4.88
0.11	0.98	0.10	0.90	5.36
0.16	1.47	0.15	1.37	6.36
0.22	2.04	0.21	1.93	7.6

TABLE B.3 AMINE FUNCTIONALIZED MEMBRANE ADSORPTION DATA WITH BSA

Abs	Co(mg/ml)	Abs	C*(mg/ml)	q*(mg/m^2)
0.02	0.19	0.02	0.14	3.36
0.03	0.31	0.17	0.25	4.23
0.07	0.57	0.07	0.48	6.00
0.08	0.72	0.40	0.60	7.73
0.10	0.91	0.57	0.78	8.73
0.13	1.14	0.73	1.00	9.33
0.18	1.62	0.28	1.47	9.77
0.24	2.17	0.42	2.02	9.93
0.31	2.78	0.51	2.64	9.92

TABLE B.4 PEG MEMBRANE ADSORPTION DATA WITH BSA

Abs	Co(mg/ml)	Abs	C*(mg/ml)	q*(mg/m^2)
0.04	0.21	0.04	0.19	1.69
0.13	0.68	0.15	0.64	2.23
0.21	1.08	0.23	1.05	2.30
0.29	1.52	0.30	1.47	3.27
0.43	2.28	0.49	2.22	4.10

TABLE B.5 BARE MEMBRANE ADSORPTION DATA WITH IgG

Abs	Co(mg/ml)	Abs	C*(mg/ml)	q*(mg/m^2)	Abs(420)
0.376	0.27	0.035	0.15	7.88	0.13
0.100	0.42	0.057	0.25	11.60	0.13
0.191	0.81	0.159	0.56	16.40	0.14
0.200	1.10	0.194	0.80	20.13	0.15
0.400	1.80	0.3642	1.48	21.60	0.18

TABLE B.6 SILICA COATED MEMBRANE ADSORPTION DATA WITH IgG

Abs	Co(mg/ml)	Abs	C*(mg/ml)	q*(mg/m^2)	Abs(420)
0.376	0.27	0.032	0.12	10.00	0.13
0.104	0.44	0.047	0.26	15.82	0.13
0.191	0.81	0.135	0.53	18.80	0.14
0.248	1.40	0.351	1.08	21.33	0.15
0.360	1.80	0.3527	1.45	23.20	0.18

TABLE B.7 AMINE FUNCTIONALIZED MEMBRANE ADSORPTION DATA WITH IgG

Abs	Co(mg/ml)	Abs	C*(mg/ml)	q*(mg/m^2)	Abs(420)
0.313	0.22	0.241	0.15	4.54	0.1
0.897	0.63	0.77	0.50	8.67	0.13
0.353	1.00	0.204	0.72	17.92	0.14
0.563	1.60	0.41	1.19	27.20	0.15
0.760	2.17	0.521	1.52	41.47	0.26

TABLE B.8 IgG DESORPTION FROM G1 MEMBRANE

	Time	C*(mg/ml)	qdes(mg/m^2)
B4 washing initially	0 min	0.52	9.83
After washing(PBS)	20 min	0.02	0.67
After washing(PBS)	20 min	0.03	1.00
Desorption-citrate	1 hr	0.039	2.60
Desorption-citrate	1 hr	0.026	1.73
Desorption-citrate	1 hr	0.02	1.33
		prot desorb	7.33
Protein recovery=	75	percent	

TABLE B.9 IgG AND BSA DESORPTION FROM G1 MEMBRANE

	Time	C*(mg/ml)	qdes(mg/m^2)
B4 washing initially	0 min	0.50	8.67
After washing(PBS)	20 min	0.024	0.80
After washing(PBS)	20 min	0.028	0.93
Desorption-citrate	1 hr	0.044	2.93
Desorption-citrate	1 hr	0.024	1.60
Desorption-citrate	1 hr	0.005	0.33
		prot desorb	6.60
protein recovery=	76	Percent	

TABLE B.10 BSA DESORPTION FROM G1 MEMBRANE

	Time	C*(mg/ml)	qdes(mg/m^2)
B4 washing initially	0 min	0.58	3.59
After washing(PBS)	20 min	0.035	1.17
After washing(PBS)	20 min	0.025	0.83
Desorption citrate	1 hr	0.027	1.80
Desorption citrate	1 hr	0.0018	0.12
Desorption citrate	1 hr	0.001	0.07
		Prot desorb	3.99
protein recovery =	100%		

TABLE B.11 IgG DESORPTION FROM G2 MEMBRANE

	Time	Abs	C*(mg/ml)	qdes(mg/m^2)
B4 washing initially	0 min	0.1979	0.57	6.87
After washing(PBS)	10 min	0.0155	0.01	0.33
After washing(PBS)	10 min	-	0	0
After washing(PBS)	10 min	-	0	0
After washing(PBS)	10 min	-	0	0
Desorption citrate	1 hr	0.003	0.005	0.33
Desorption citrate	1 hr	0.01	0.015	1.00
Deadsorption NaCl	15 min	-	0	0.00
left in PBS buffer	2 days	0.0038	0.003	0.20
Desorption-citrate	30 min	-	0.018	1.20
Desorption-citrate	19 hrs.	0.0043	0.006	0.40
			Prot desorb	3.47

TABLE B.12 BSA DESORPTION FROM G2 MEMBRANE

	Time	Abs		
B4 washing initially	0 min	0.10	C*(mg/ml)	qdes(mg/m^2)
After washing(PBS)	10 min	0.0061	0.63	0.67
After washing(PBS)	10 min	0.0029	0.01	0.33
After washing(PBS)	10 min	0.0017	0.0045	0.15
After washing(PBS)	25 min	-	0.001	0.03
Deadsorption Citrate	1 hr	0.018	0	0.00
Deadsorption Citrate	1 hr	-	0.009	0.60
Deadsorption Citrate	14 hrs	-	0	0.00
			prot deads	1.12

TABLE B.13 IgG DESORPTION FROM G3 MEMBRANE

	Time	C*(mg/ml)	qdes(mg/m^2)
B4 washing initially	0 min	0.51	14.96
After washing(PBS)	20 min	0.054	1.80
After washing(PBS)	20 min	0.054	1.80
Desorption citrate	1 hr	0.049	3.27
Desorption citrate	1 hr	0.026	1.73
Desorption citrate	1 hr	0.012	0.80
		Prot desorb	9.40
Protein recovery=	63	Percent	

TABLE B.14 IgG AND BSA DESORPTION FROM G3 MEMBRANE

	Time	C*(mg/ml)	qdes(mg/m^2)
B4 washing initially	0 min	0.38	15.03
After washing(PBS)	20 min	0.0177	0.59
After washing(PBS)	20 min	0.0116	0.39
Deadsorption NaCl	1 hr	0.004	0.27
Desorption citrate	1 hr	0.038	2.53
Desorption citrate	1 hr	0.028	1.87
Desorption citrate	1 hr	0.015	1.00
		prot desorb	6.64
protein recovery=	44	Percent	

TABLE B.15 BSA DESORPTION FROM G3 MEMBRANE

	Time	C*(mg/ml)	qdes(mg/m^2)
B4 washing initially	0 min	0.63	1.01
After washing(PBS)	20 min	0.0023	0.08
After washing(PBS)	20 min	0.009	0.30
Deadsorption NaCl	1 hr	0	0.00
Desorption citrate	1 hr	0.011	0.73
Desorption citrate	1 hr	0.0012	0.08
Desorption citrate	1 hr	0	0.00
		Prot desorb	1.19
protein recovery =	100%		

VITA

Name:	Tahmina Imam
Address:	Mayview Community Health Center Shamima Hasan 270 Grant Avenue Palo Alto, CA 94306, USA
Email Address:	nisha4433@yahoo.com
Education:	B.S., Chemical Engineering, San Jose State University, 2006 M.S., Chemical Engineering, Texas A&M University, 2009